gLLP

(NASA-TM-X-71527) PRELIMINARY MEASUREMENT OF THE AIRFRAME NOISE FROM AN F-106B DELTA WING AIRCRAFT AT LOW FLYOVER SPEEDS (NASA) ~~42~~ 44 p HC $5.25 CSCL 01C

N74-19668

Unclas

G3/02 34368

NASA TECHNICAL MEMORANDUM

NASA TM X-71527

NASA TM X-71527

PRELIMINARY MEASUREMENT OF THE AIRFRAME NOISE FROM AN F-106B DELTA WING AIRCRAFT AT LOW FLYOVER SPEEDS

by Richard R. Burley
Lewis Research Center
Cleveland, Ohio 44135
March 1974

This information is being published in preliminary form in order to expedite its early release.

E-7928

ABSTRACT

To establish a realistic lower limit for the noise level of advanced supersonic transport aircraft will require knowledge concerning the amount of noise generated by the airframe itself as it moves through the air. The airframe noise level of an F-106B aircraft was determined and was compared to that predicted from an existing empirical relationship. The data were obtained from flyover and static tests conducted to determine the background noise level of the F-106B aircraft. Preliminary results indicate that the spectrum associated with airframe noise was broadband and peaked at a frequency of about 570 hertz. An existing empirical method successfully predicted the frequency where the spectrum peaked. However, the predicted OASPL value of 105 dB was considerably greater than the measured value of 83 dB.

E-7928

PRELIMINARY MEASUREMENT OF THE AIRFRAME NOISE FROM AN F-106B DELTA WING AIRCRAFT AT LOW FLYOVER SPEEDS

by Richard R. Burley

Lewis Research Center

SUMMARY

To establish a realistic lower limit for the noise level of advanced supersonic transport aircraft will require knowledge concerning the amount of noise generated by the airframe itself as it moves through the air. The airframe noise level of an F-106B aircraft was determined and was compared to that predicted from an existing empirical relationship. The data were obtained from flyover and static tests conducted to determine the background noise level of the F-106B aircraft, which is a delta wing aircraft designed for supersonic speeds. The flyover tests were conducted at an altitude of 91 meters (300 ft) at a Mach number of 0.4. The main engine was at idle power and the landing gear was retracted.

Preliminary results indicate that the spectrum associated with airframe noise was broadband and peaked at a frequency of about 570 hertz. An existing empirical method successfully predicted the frequency where the spectrum peaked. However, the predicted OASPL value of 105 dB was considerably greater than the measured value of 83 dB.

INTRODUCTION

A major effort has gone into the development of jet exhaust suppressors and acoustically treated nacelles directed at quieting the engine noise of advanced supersonic transport aircraft. This has led to predictions that aircraft noise levels considerably below current FAR-36 requirements can be achieved (ref. 1). However, it has recently been suggested (ref. 2) that a noise floor exists below which quieting the engines will be ineffective.

A principle source of this noise floor is the airframe itself as it moves through the air. Some studies of this noise source have been done using aircraft designed for subsonic speeds (refs. 2 and 3). However, since aircraft designed for supersonic speeds have a significantly different shape, airframe noise could be considerably different. Thus, an important question concerns the airframe noise of aircraft designed for supersonic speeds.

To gain some insight into this question, the airframe noise level of an F-106B aircraft was determined and was compared to that predicted from the existing empirical relationships of reference 2. The data were obtained from flyover and static tests conducted to determine the background noise level of the F-106B aircraft. These tests were part of an investigation of the effect of flight velocity on the jet noise and thrust associated with unsuppressed and suppressor type exhaust nozzles (refs. 4 to 11).

The F-106B is a delta wing aircraft designed for a maximum speed of Mach 2 in level flight. The flyovers were conducted at an altitude of 91 meters (300 ft) and a Mach number of 0.4. The landing gear was retracted for these tests. Acoustic measurements were taken from a ground station directly beneath the flight path. For the static tests, the acoustic measurements were taken at a radial distance of 30.48 meters (100 ft) from the nozzle. The main engine of the aircraft, a J75, was at idle power for both the flyover and the static tests.

SYMBOLS

b	wing span, m (ft)
C	average wing chord, m (ft)
c_L	coefficient of lift
h	aircraft altitude, m (ft)
OASPL	overall sound pressure level, dB(re 2×10^{-5} N/m^2)
PNL	perceived noise level, PNdB
R_p	direct ray distance between exhaust nozzle and microphone, m (ft)
t	wing thickness/2, cm (in.)
t_m	mean wing thickness, m (ft)
V	aircraft velocity, meters/sec (ft/sec)
W	aircraft gross weight, kg (lbm)
x	distance on strut measured aft of strut fairing leading edge, cm (in.)
x_n	distance on nacelle measured aft of inlet lip, cm (in.)
x_w	distance along wing chord line measured aft from point of intersection of inlet lip plane and wing chord, cm (in.)
y	distance from aircraft centerline to nacelle centerline, m (in.)
δ	elevon deflection, deg
θ	angle between direct ray and jet exit centerline, deg

APPARATUS AND PROCEDURE

Aircraft

The tests were conducted with an F-106B aircraft modified to carry two underwing nacelles. Figure 1 shows the aircraft in flight. Table I gives dimensional data of the aircraft and figure 2 shows a schematic drawing of the aircraft details and installation of the nacelles. The aircraft was 20.076 meters (790.4 in.) long and had a 60° sweptback delta planform with a 5.812-meter (228.8-in.) semispan. The wing had an approximately 4 percent thick NACA 0004-65 airfoil section with a cambered leading edge, a mean aerodynamic chord of 7.24 meters (285 in.), and an aspect ratio of 2.2. The nacelles were mounted to the wing aft lower surface by two attachment links (which were enclosed by strut fairings) on each side of the fuselage at a spanwise distance (y) of 1.863 meters (73.34 in.) or about 32 percent semispan. The nacelles were inclined 4.5° down with respect to the wing chord line so that the aft portion of the nacelle would be tangent to the lower surface of the wing at its trailing edge (fig. 2(b)). The nacelles extended below the fuselage lower surface which is fairly flat in the region of the nacelles. Because of transonic area rule considerations, the fuselage sidewalls on the bottom have a slight contour in the vicinity of the nacelles (fig. 2(a)).

A schematic drawing of the nacelle strut fairing and elevon is shown in figure 3. The strut fairing tapered to a maximum width of 57 percent of the nacelle diameter near the elevon hinge line. A gap of 0.64 centimeter (0.25 in.) was maintained between the lower wing surface and the fairing. The struts were mounted directly to the nacelles. A 62.23-centimeter (24.5-in.) wide section of each elevon immediately above the nacelles was cut out and rigidly fixed to the wing to provide clearance between the movable elevon and nacelle (fig. 3(b)).

A schematic drawing of the nacelle is presented in figure 4. Each nacelle, which has a cylindrical diameter of 63.5 centimeters (25 in.) and is 452.55 centimeters (178.17 in.) long, contains a calibrated J85-GE-13 afterburning turbojet engine. The flat-bottomed bulge on the nacelle shown in sections A-A and B-B was needed to accommodate the J85 engine accessory package.

Noise Measurements

Microphones for both flyover and static tests were 2.54 centimeters (1 in.) diameter ceramic type. Their frequency response were flat to within ±2 dB for grazing incidence over the frequency range used (50 to 10 KHz). The output of the microphones was recorded on a two-channel direct record tape recorder. The entire system was calibrated for sound level in the field before and after each test with a conventional tone calibrator. The tape recorder was calibrated for linearity with a "pink" noise (constant energy per octave) generator.

Both the flyover and the static signals were recorded on magnetic tape. The tape was played back through one-third-octave-band filters and then reduced to digital form. The averaging time for data reduction was 0.1 second for the flyover signal and 0.125 second for the static signal.

Meteorological conditions, in terms of dry-bulb and dew point temperatures, wind speed and direction, and barometric pressure were recorded periodically throughout the tests. Wind speeds were less than 5.144 meters per second (10 knots) during all tests.

Noise measurements for the flyover tests were made from a ground station under the flight path (fig. 5(a)). The microphone, which was fitted with a wind screen that caused no loss of signal, was positioned 1.22 meters (4 ft) above a concrete surface. It was oriented to receive the acoustic pressure wave at grazing incidence.

The geometry of the flyover is shown in figure 5(b). As the aircraft travels along its flight path, the direct ray distance from the nozzle to the microphone, R_p, continuously changes. The angle between the direct ray and the jet exit centerline, referred to as the acoustic angle θ, also changes. The values of R_p and θ shown in figure 5(b) assumes the aircraft flys directly over the microphone at an altitude of exactly 91 meters (300 ft). But since this may not always be the case, provisions were made to adjust the recorded sound pressure level to these conditions. This was accomplished with the aid of a signal recorded on the tape. At the same time a photograph was taken from a ground based camera of the aircraft as it was passing overhead. Details are given in reference 11.

The flyovers were conducted at a Mach number of 0.4. The main engine of the aircraft (a J75) was at idle power while the data were being recorded; both J85 engines were shut off and allowed to windmill.

The location of the microphone for static tests is shown in figure 6. It was positioned 1.22 meters (4 ft) above a concrete surface and was oriented to receive the acoustic pressure wave at normal incidence (fig. 6(a)). It was fitted with a windscreen that caused no loss of signal. The acoustic measurements were taken at a radial distance of 30.48 meters (100 ft) from the nozzle exit in increments of 10° over a 90° sector (fig. 6(b)). During the measurements, the main engine was at idle power and both J85 engines were shut off.

RESULTS AND DISCUSSION

Airframe Noise

The F-106B aircraft was flown over the noise measuring station at an altitude of 91 meters (300 ft) with its main engine (J75) at idle power and both J85 engines shut off and windmilling. Sources of noise were the compressors and turbines of all engines, the turbulent mixing of the exhaust jets with the surrounding air, and the airframe. Since noise sources other than the airframe are readily identifiable, airframe noise is defined as what remains after accounting for these other noise sources.

The noise sources are identified from either flyover or static spectra that have been adjusted to free-field conditions on a standard day. The static spectra were further adjusted from the 30.48-meter (100-ft) radius at which the data were taken to the 91-meter (300 ft) sideline conditions of the flyover. Details of the adjustments are given in reference 6. In examining the flyover spectra, the greatest emphasis should be placed on the data at frequencies between 160 and 5000 hertz. At frequencies below 160 hertz, the short integration time, the narrowness of the frequency bands, and the changing conditions of the flyover combine to give results that are less reliable. At frequencies above 5000 hertz, the acoustic signal received at the measuring station quite possibly is below the noise floor of the recording equipment.

The frequency spectrum at flyover conditions is shown in figure 7 for acoustic angles in the region of peak flyover noise. The segment of the spectrum between frequencies of 200 and 1250 hertz is considered to be due to airframe noise. It is broadband with a peak value of 73 dB occurring at a frequency of about 570 hertz.

The mid-to-high frequency portion of the spectra shown in figure 7 is due to discrete tones from the engines. These tones along with the other non-airframe noise sources will be discussed later.

Comparison with Predictions

An empirical method was developed in reference 2 for predicting airframe noise. It was based on tests of five aircraft designed for low subsonic speeds. The aircraft were a Prue-2 sailplane, Cessna 150, Aero Commander, Douglas DC-3, and a Convair 240, covering a gross weight range from 590 to 17 700 kilograms (1300 to 39 000 lb). Airspeed varied from 30 to 99 meters per second (58 to 192 knots). The resulting empirical relationship for overall sound pressure level of an aerodynamically "clean" configuration was:

$$\mathrm{OASPL} = 10\ \mathrm{LOG}_{10}\left[2.92 \times \frac{V^4}{h^2} \times \frac{W}{c_L} \times \frac{C}{b}\right] + 8.4,\ \mathrm{dB}$$

Since gross weight, W, is essentially equal to lift which is proportional to the second power of velocity, the OASPL is proportional to the sixth power of velocity. The measured spectrum was broadband and peaked at a frequency given by:

$$f = 1.097 \times \frac{V}{t_m},\ \mathrm{Hz}$$

(Dimensions as given in SYMBOLS.) Since airfoil thickness, t_m, was found to be the relevant length factor in the Strouhal number and because of the dipole nature of the noise (i.e., V^6), it was concluded that the predominant noise source was wing trailing edge vortex shedding.

How successful these relationships are in predicting the airframe noise of an F-106B delta wing aircraft designed for supersonic speeds is shown in figure 8. The segment of the airframe spectrum (see fig. 7) has been extrapolated and OASPL and PNL values calculated. These values along with the predicted OASPL value are shown in the table. Also shown in the table is the frequency where the spectrum peaked along with the predicted value.

The empirical relationship successfully predicted the frequency at which the broadband spectrum peaked. This suggests that the predominant noise source from the F-106B airframe was due to wing trailing edge vortex shedding. The empirical relationship was not successful in predicting the level of the sound. The predicted OASPL value of 105 dB was considerably higher than the measured value of 83 dB. This suggests that a delta wing may result in relatively weak vortex shedding noise or that airframe noise might not vary with the sixth power of aircraft velocity. Also the aircraft from which the empirical equation was obtained were not as aerodynamically clean as the F-106B aircraft.

Another estimate of airframe noise is given in reference 3. Flight tests of 727 and 747 aircraft identified airframe noise levels for these aircraft approximately 8 E PNdB below current FAR 36 standards. The results were then extrapolated to cover a range of gross weights from about 13 700 to 410 000 kilograms (30 000 to 900 000 lb). The tests also showed that E PNdB varied as about the fourth power of aircraft velocity.

The tests were done for approach conditions, that is for a Mach number of 0.23 at an altitude of 113 meters (370 ft). For these conditions, and for an aircraft with the same gross weight as that of the F-106B aircraft (17 000 kg), the airframe noise level was estimated to be about 93 E PNdB from reference 3.

To compare with the F-106B results, the 93 E PNdB estimated noise level was converted from E PNdB to PNdB and then adjusted to the flyover conditions of the F-106B aircraft (i.e., a Mach number of 0.4 at an altitude of 91 m). An increase of 3 PNdB was applied to convert from E PNdB to PNdB (ref. 12). Another 10 PNdB was added to account for the increase in aircraft speed from 0.23 to 0.04 Mach number (noise was assumed to increase with the fourth power of aircraft speed). Finally, 2 PNdB was added to account for the reduction in altitude from 113 to 91 meters. This resulted in a predicted airframe noise level of 108 PNdB. The measured airframe noise level is considerably lower at a value of 94 PNdB (fig. 8).

Thus, preliminary results indicate that the amount of noise generated by the airframe of an F-106B aircraft as it moves through the air is considerably below predicted values. Although the reasons are not yet known, there are several significant differences between the present tests and those of references 2 and 3. One difference is the wing planform of the aircraft; the F-106B aircraft has a low aspect ratio delta wing whereas the other aircraft have relatively high aspect ratio tapered or swept back wings. A second difference is the lift coefficient at low subsonic speeds; the F-106B aircraft has a relatively low lift coefficient compared to the other aircraft. A third difference is the flight speed at which the tests were conducted; the F-106B aircraft was flown at a considerably higher speed than the other aircraft. A fourth difference is the flight path; the F-106B aircraft was flown at a constant altitude whereas at least some of the other aircraft were flown along a glide path simulating approach conditions.

Non-Airframe Noise

As mentioned, identifying airframe noise requires determining the non-airframe noise sources. One of these sources is discrete tones due to the rotational speed of the engines. These tones occur at frequencies corresponding to blade passing frequencies of the turbine as well as the first few stages of the compressor. The fundamental frequency, which is determined by the product of the number of rotor blades in a stage and its rotational speed, is shown in table II.

These tones are responsible for the noise in the mid-to-high frequency portion of the flyover spectra shown in figure 7. The J85 engine contributed tones in the mid frequencies; compressor tones occurred at frequencies of about 1800, 3500, and 5100 hertz and turbine tones occurred at frequencies of about 3200 and 4400 hertz. The J75 engine contributed tones in both the mid and high frequencies; compressor tones occurred at frequencies of about 2500 and 2800 hertz and turbine tones occurred at frequencies of about 7200, 8700, and 9400 hertz.

The other non-airframe noise source is broadband noise emerging from the exhaust nozzle. For the J75 engine, which operates at idle power, broadband noise consists of combustion, turbomachinery, and jet mixing noise. The noise was identified from tests conducted at static conditions. The spectrum is shown in figure 9(a) for the acoustic angles that resulted in peak flyover noise. Broadband noise reached a peak value of 65 dB at a frequency of about 125 hertz. The spikes at frequencies above 1 kHz were probably caused by the rotating machinery.

Noise from the J75 engine at idle power does not significantly influence airframe noise. This is shown in figure 9(b) where the noise level of the J75 engine is at least 10 dB below airframe noise except at the low frequencies (about 200 Hz).

Broadband noise also emerges from the exhaust nozzle of the J85 engine. It is also low enough so as not to influence airframe noise. Since the J85 engine is shut off and windmilling rather than operating at idle power as is the J75 engine, the noise consists of turbomachinery noise and jet mixing noise but no combustion noise. Because the exhaust jet is not heated, jet velocity and, consequently, jet mixing noise will be lower than that from the J75 engine. Thus, the broadband noise from the J85 engine will be lower than that from the J75 engine which is itself insignificant in the frequency range of interest.

Directivity and Spectra

The results of the flyover tests conducted at an altitude of 91 meters (300 ft) are shown in figure 10 in terms of the variation in overall sound pressure level (fig. 10(a)) and perceived noise level (fig. 10(b)) as a function of acoustic angle. Also shown are the results of the static tests (J75 engine at idle power and J85 engines off) adjusted to the 91-meter (300-ft) sideline conditions of the flyover.

The flyover noise level reached a peak value of 87 dB (98 PNdB) at an acoustic angle of about 110°. The peak noise level is fairly flat changing less than 1 dB between acoustic angles of 130° and 90°. This is in agreement with reference 2 in which the peak noise level was obtained at 90°.

The static noise level was fairly flat at a value of 75 dB (87 PNdB) between acoustic angles of 100° and 80°. This level is at least 10 dB below the corresponding flyover level indicating again that the J75 engine at idle power does not significantly influence the flyover noise level. The static noise level then increased and reached a peak value of 78 dB (89 PNdB) at an acoustic angle of 60°. At lower acoustic angles, the static and flyover curves are parallel. The level of the static curve is only 5 dB below the corresponding flyover curve indicating that now the J75 engine makes a significant contribution to the flyover noise.

The sound pressure level values just discussed were determined from frequency spectra. These spectra are presented in figure 11 for acoustic angles between 120° and 30° in increments of 10°. At angles between 100° and 30°, both flyover and static spectra are given; at angles of 120° and 110°, the flyover spectra is shown.

SUMMARY OF RESULTS

The airframe noise level of an F-106B aircraft was determined and was compared with that predicted from an existing empirical relationship. The data were obtained from flyover and static tests conducted to determine the background noise level of the F-106B aircraft, which is a delta wing aircraft designed for supersonic speeds. The flyover tests were conducted at an altitude of 91 meters (300 ft) and a Mach number of 0.4. The main engine was at idle power and the landint gear was retracted. Preliminary results of the investigation can be summarized as follows:

1. The spectrum associated with airframe noise is broadband and peaks at a frequency of about 570 hertz.

2. An existing empirical method successfully predicted the frequency at which the spectrum peaked. However, the predicted OASPL values of 105 dB was considerably greater than the measured value of 83 dB.

3. The noise during flyover peaked at an angle of about 110° from the jet axis. The peak was fairly flat between angles of 120° and 90°. This is in good agreement with reference 2 in which the peak noise level was obtained at 90°.

REFERENCES

1. Joint DOT-NASA Civil Aviation Research and Development Policy Study. NASA SP-265, 1971.
2. Gibson, J. S.: The Ultimate Noise Barrier - Far Field Radiated Aerodynamic Noise. In: Inter-Noise 72; International Conference on Noise Control Engineering, Washington, D.C., October 4-6, 1972, pp. 332-337.
3. Blumenthal, V. L.; Streckenbach, J. M.; and Tate, R. B.: Aircraft Environmental Problems. Jour. Aircraft, vol. 10, no. 9, Sept. 1973, pp. 529-537.
4. Burley, Richard R.; and Karabinus, Raymond J.: Flyover and Static Tests to Investigate External Flow Effects on Jet Noise for Non-Suppressor and Suppressor Exhaust Nozzles. NASA TM X-68161, 1972.
5. Brausch, J. F.: Flight Velocity Influence on Jet Noise of Conical Ejector, Annular Plug, and Segmented Suppressor Nozzles. General Electric Co. (NASA CR-12061), Aug. 1972.
6. Burley, Richard R.; Karabinus, Raymond J.; and Freedman, Robert J.: Flight Investigation of Acoustic and Thrust Characteristics of Several Exhaust Nozzles Installed on Under-Wing Nacelles on an F106 Airplane. NASA TM X-2854, 1973.
7. Chamberlin, Roger: Flyover and Static Tests to Study Flight Velocity Effects on Jet Noise of Suppressed and Unsuppressed Plug Nozzle Configurations. NASA TM X-2856, 1973.
8. Burley, Richard R.; and Johns, Albert L.: Flight Velocity Effects on Jet Noise of Several Variations of a Twelve-Chute Suppressor Installed on a Plug Nozzle. NASA TM X-2918, 1974.

9. Burley, Richard R.; and Head, Verlon L.: Flight Velocity Effects on Jet Noise of Several Variations of a 48-Tube Suppressor Installed on a Plug Nozzle. NASA TM X-2919, 1974.

10. Wilcox, Fred A.: Comparison of Ground and Flight Test Results Using a Modified F106B Aircraft. NASA TM X-71439, 1973.

11. Burley, Richard R.: Flight Velocity Effects on the Jet Noise of Several Variations of a 104-Tube Suppressor. NASA TM X-3049, 1974.

12. Tanner, Carole S.; and Glass, Roy E.: Analysis of Operational Noise Measurements in Terms of Selected Human Response Noise Evaluation Measures. Hydrospace Research Corp. (FAA-RD-71-112), 1971.

TABLE I.- DATA FOR UNMODIFIED AIRCRAFT (EXCLUDES NACELLES)

WING	
AIRFOIL SECTION	NACA 0004-65 (MOD.)
SPAN	11.62 m
AREA (TO AIRCRAFT ℄)	64.33 m^2
ROOT CHORD (AT AIRCRAFT ℄)	10.86 m
TIP CHORD	0.29 m
MEAN AERODYNAMIC CHORD	7.24 m
ASPECT RATIO	2.2
TAPER RATIO	0
SWEEPBACK OF LEADING EDGE	60°
SWEEPBACK OF TRAILING EDGE	-5°
ELEVONS	
TYPE	PLAIN (RADIUS NOSE)
SPAN	3.92 m
AREA AFT OF HINGE LINE	6.2 m^2
ROOT CHORD	0.96 m
TIP CHORD	0.62 m
VERTICAL TAIL	
AIRFOIL SECTION	NACA 0004-65 (MOD.)
AREA (TOTAL)	9.8 m^2
ASPECT RATIO	0.97
SWEEPBACK OF LEADING EDGE	55°
SWEEPBACK OF TRAILING EDGE	20°
FUSELAGE	
LENGTH (OVERALL)	21.56 m
HEIGHT (MAXIMUM)	2.29 m
WIDTH (MAXIMUM)	2.47 m
SURFACE AREA	91.5 m^2
TOTAL AIRPLANE SURFACE AREA	207.2 m^2
GROSS WEIGHT (INCLUDES NACELLES)	17,000 kg

TABLE II.- FUNDAMENTAL BLADE PASSING FREQUENCY.

				BLADE PASSING FREQ., Hz		
		% RPM	RPM	FIRST STAGE	SECOND STAGE	THIRD STAGE
COMP.	J-75	60 (IDLE)	5239	2445	2445	2794
COMP.	J-85	WIND-MILL	3500	1808	3500	5075
TURBINE	J-75	60 (IDLE)	5239	9431	8732	7160
TURBINE	J-85	WIND-MILL	3500	4360	3200	

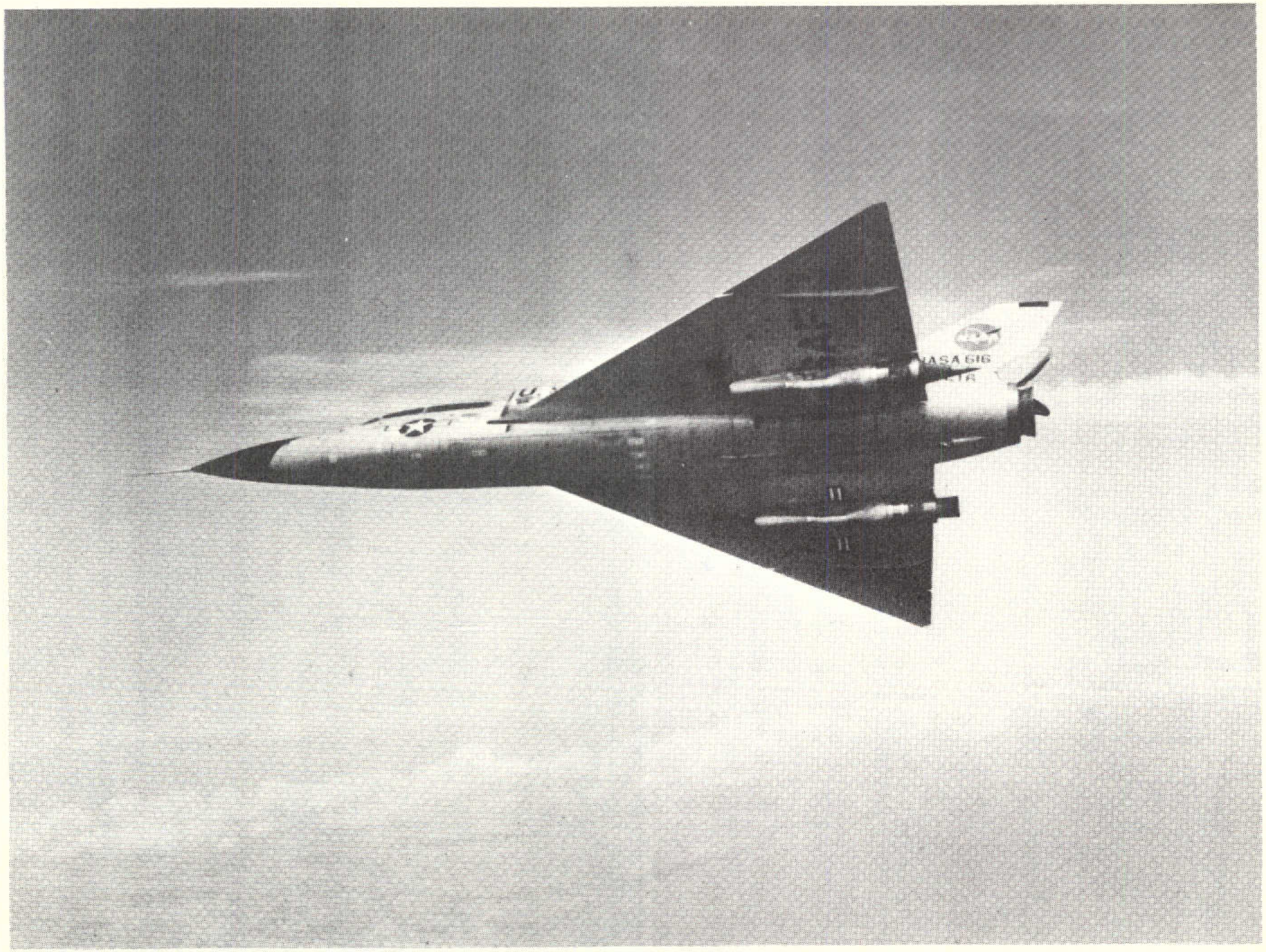

Figure 1. - Modified F-106B aircraft in flight.

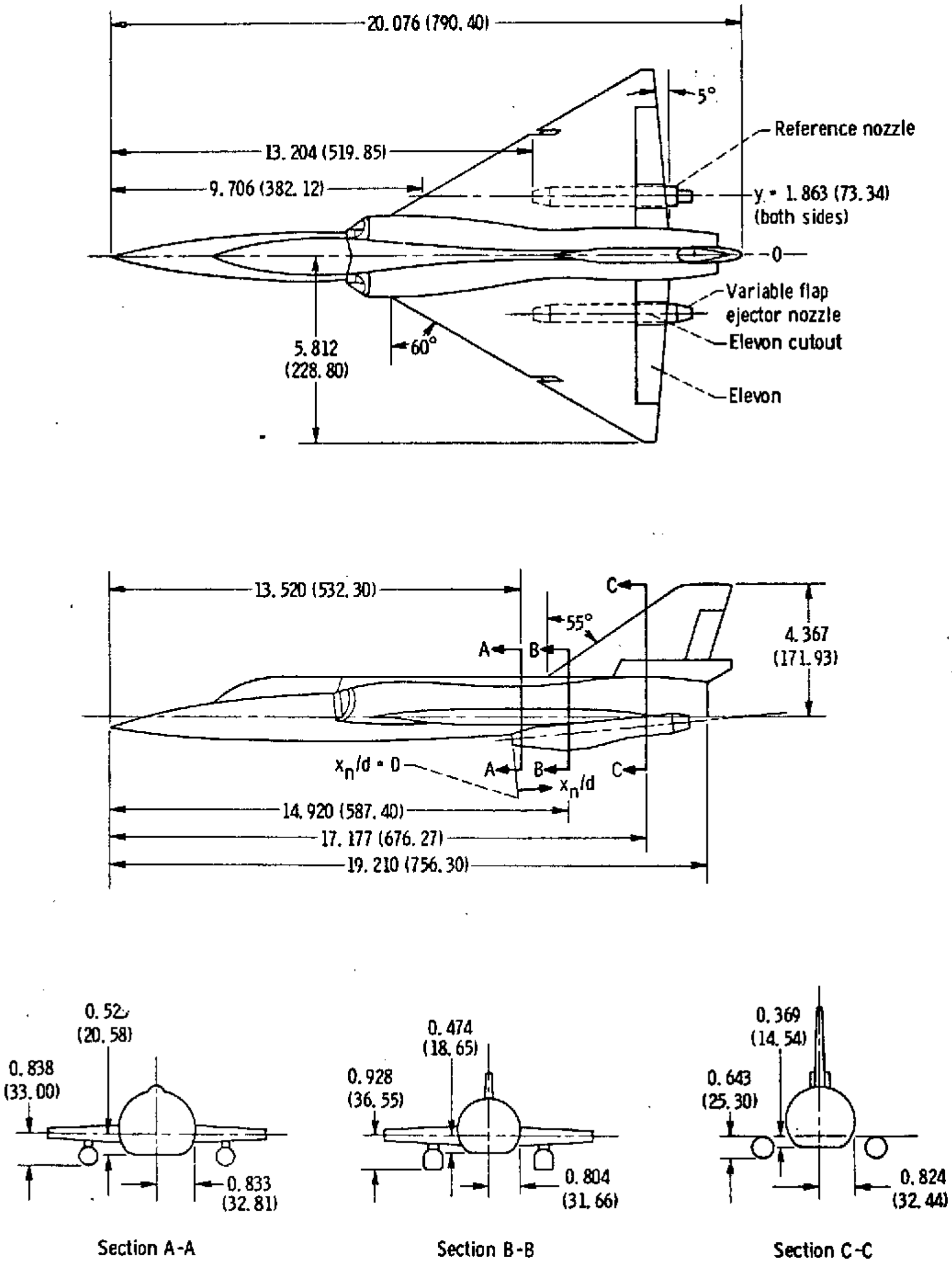

(a) Aircraft details.

Figure 2. - Aircraft details and installation of nacelles under the wing. (All dimensions in m (in.) unless indicated otherwise.)

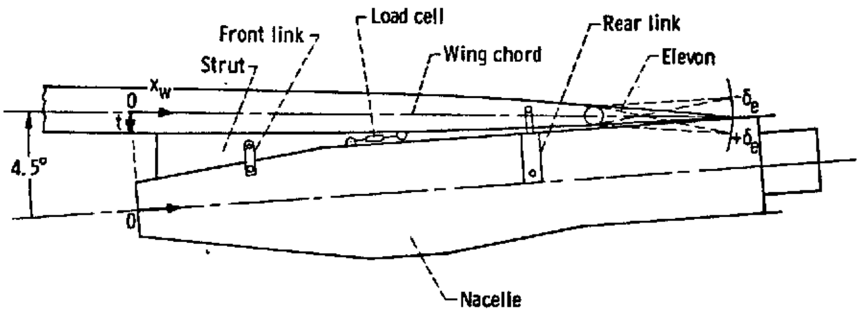

Wing lower-surface coordinates (d = 63.50 cm or 25.00 in.)			
x_w/d	t/d	x_w/d	t/d
0.	0.225	3.613	0.166
.338	.226	4.202	.145
1.069	.225	4.754	.107
2.282	.218	5.402	.062
2.802	.196	6.257	.004

(b) Nacelle installation.

Figure 2. - Concluded.

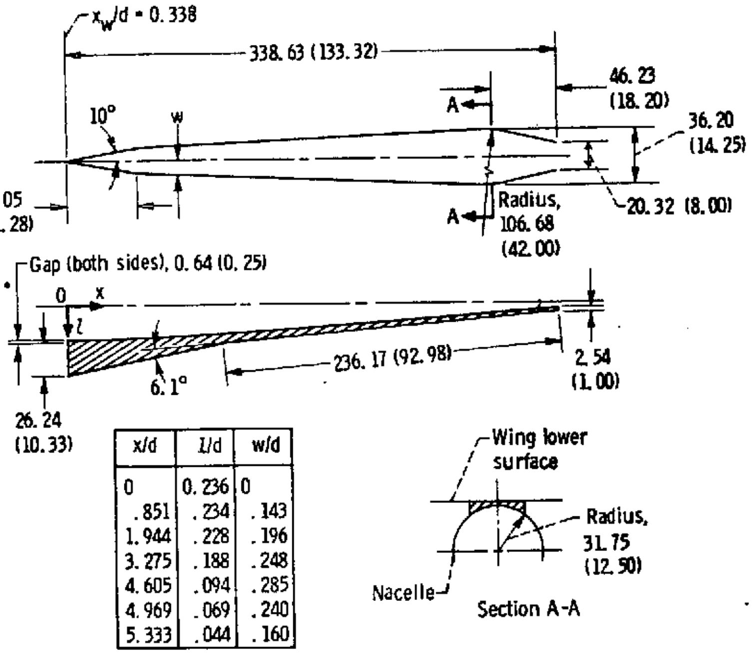

x/d	l/d	w/d
0	0.236	0
.851	.234	.143
1.944	.228	.196
3.275	.188	.248
4.605	.094	.285
4.969	.069	.240
5.333	.044	.160

(a) Wide nacelle strut fairing.

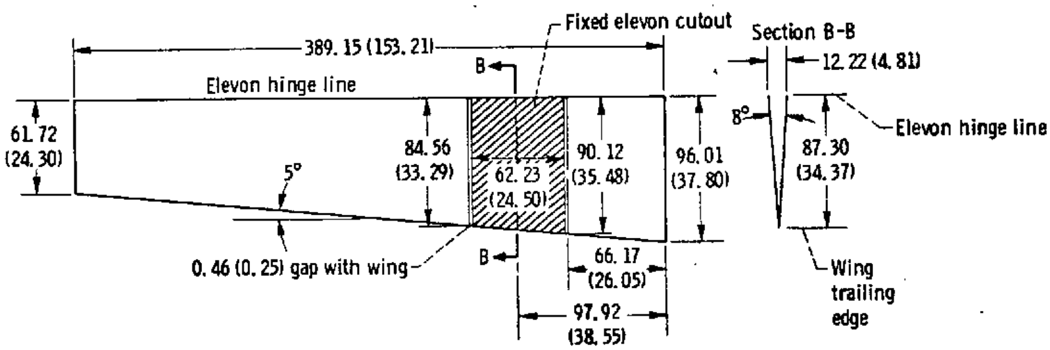

Section B-B

	x_w/d	x_n/d
Elevon hinge line	4.912	4.945
Wing trailing edge	6.290	6.240

(b) Elevon.

Figure 3. - Nacelle strut fairings and elevon. (All dimensions in cm (in.) unless indicated otherwise.)

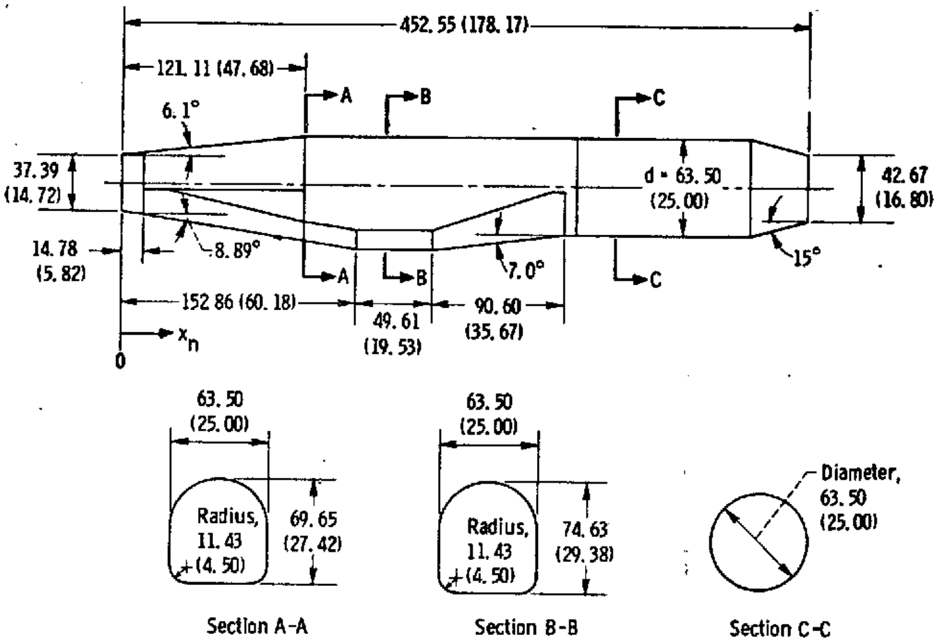

Figure 4. - Nacelle. (All dimensions in cm (in.) unless indicated otherwise.)

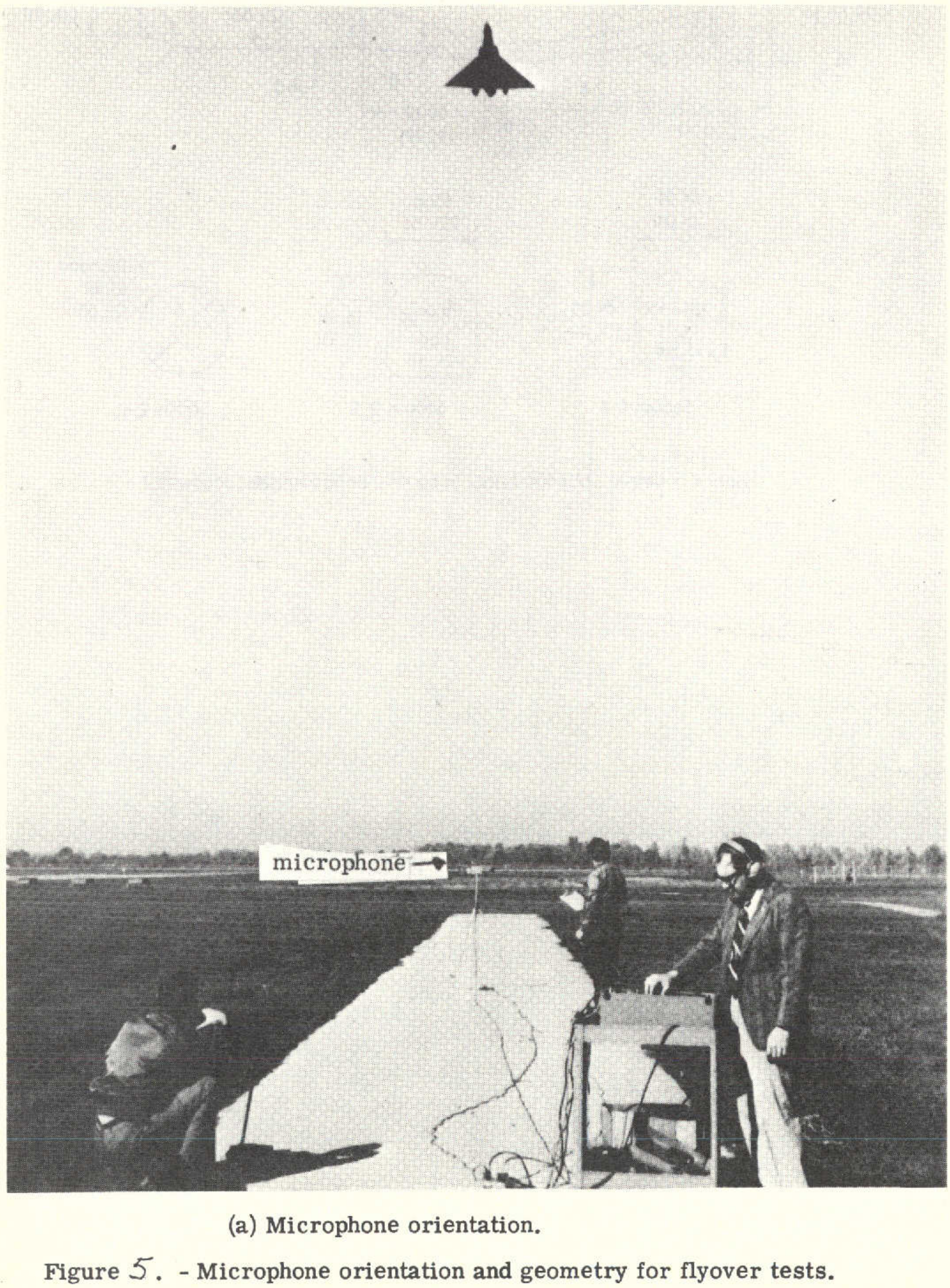

(a) Microphone orientation.

Figure 5. - Microphone orientation and geometry for flyover tests.

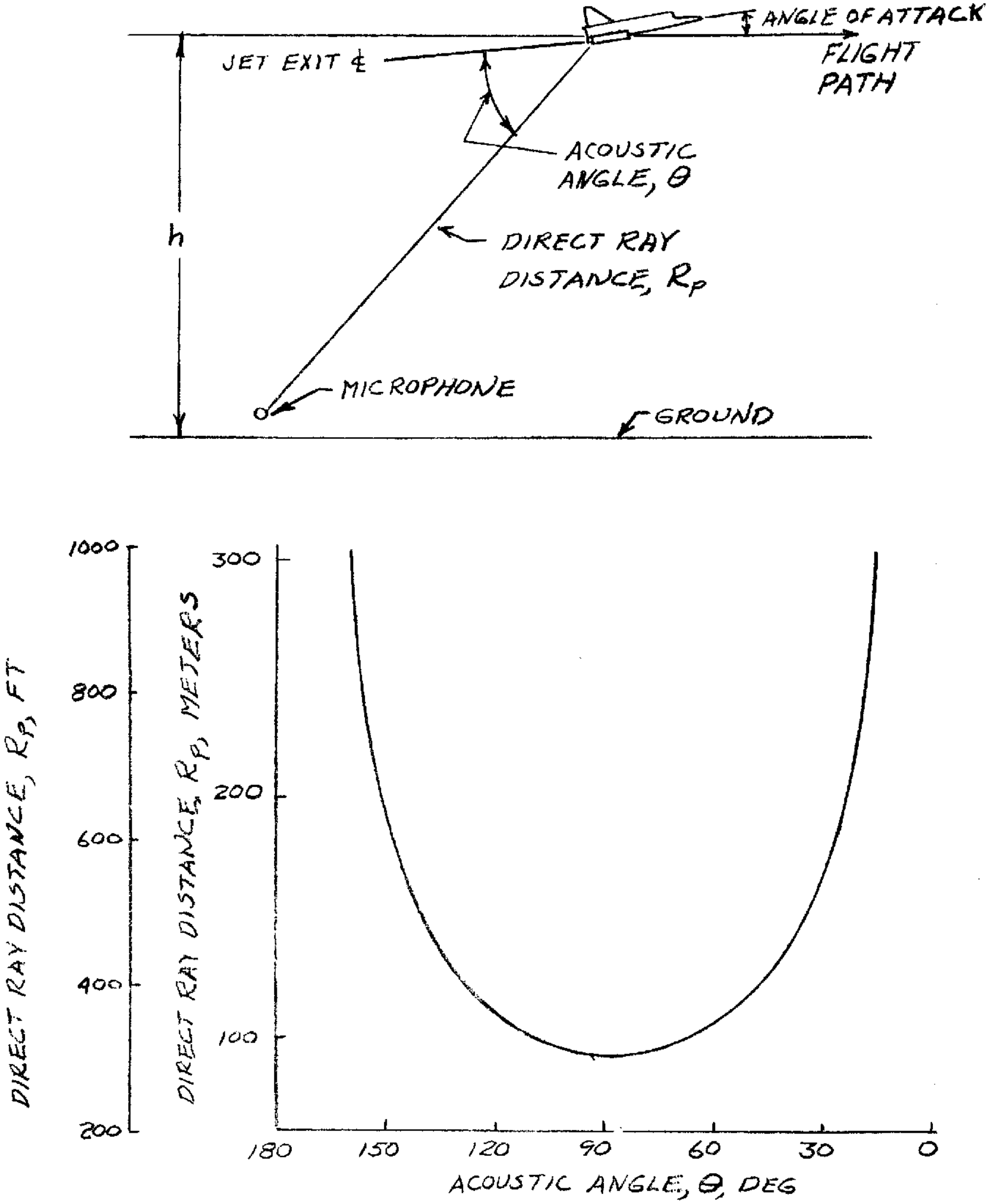

(b) GEOMETRY

FIGURE 5.- CONCLUDED

(a) Microphone orientation.

Figure 6. - Microphone orientation and location for static tests.

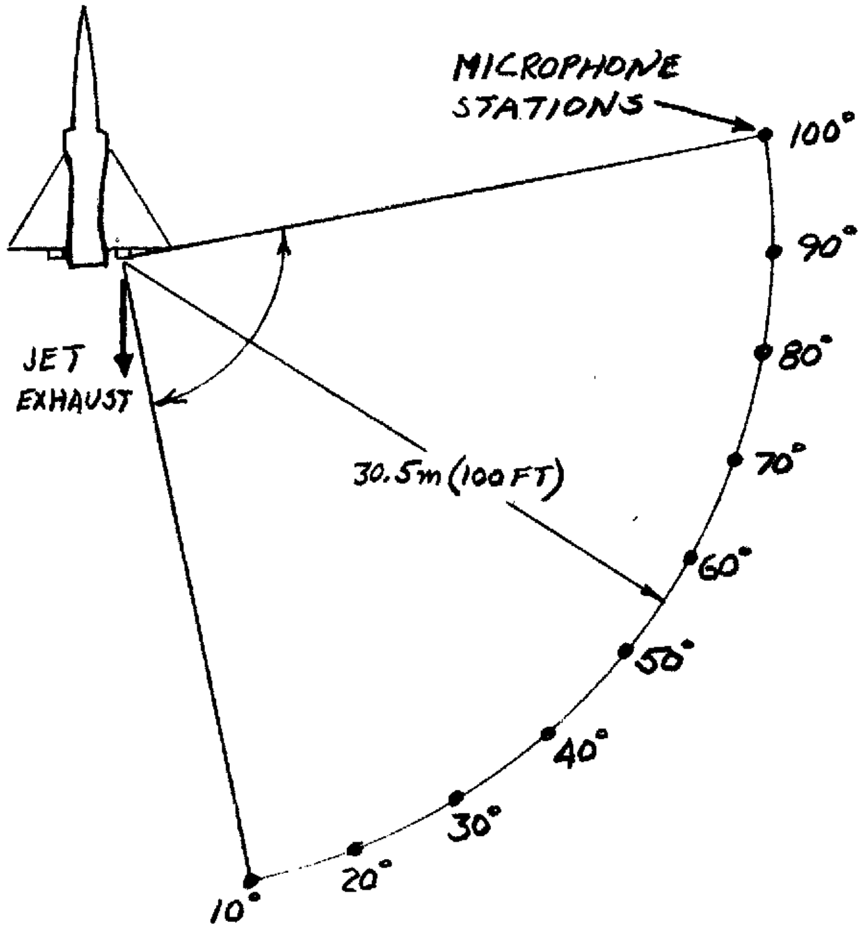

(b) MICROPHONE STATIONS

FIGURE 6.- CONCLUDED

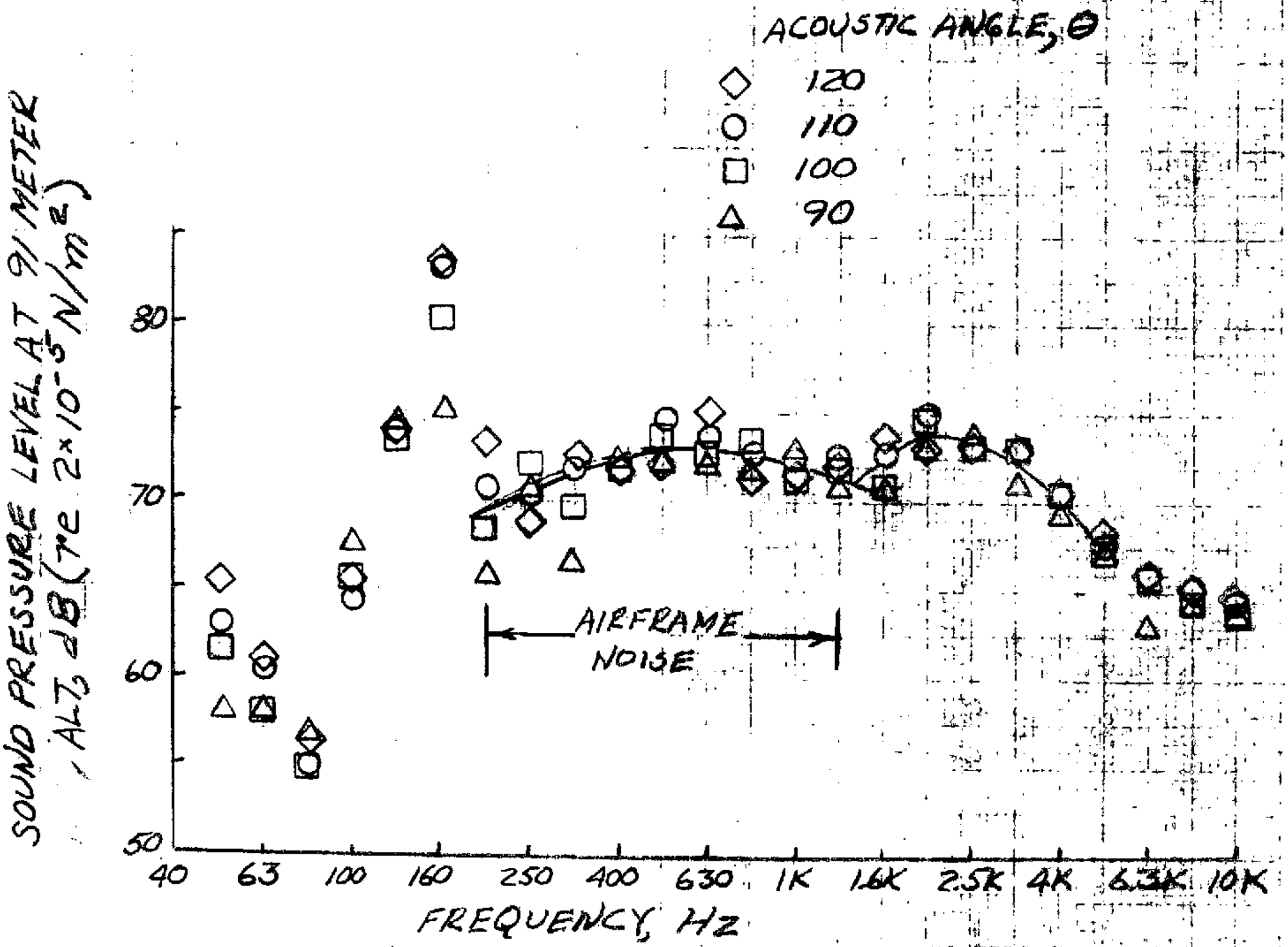

FIGURE 7.- THIRD-OCTAVE-BAND SPECTRA OF PEAK NOISE FOR FLYOVER

	OASPL, dB	PNL, PNdB	PEAK FREQ., Hz
FLIGHT DATA, F-106	83①	94①	570
CALC. FROM EQ., REF. 2	105	—	590

① ADJUSTED TO FREE-FIELD

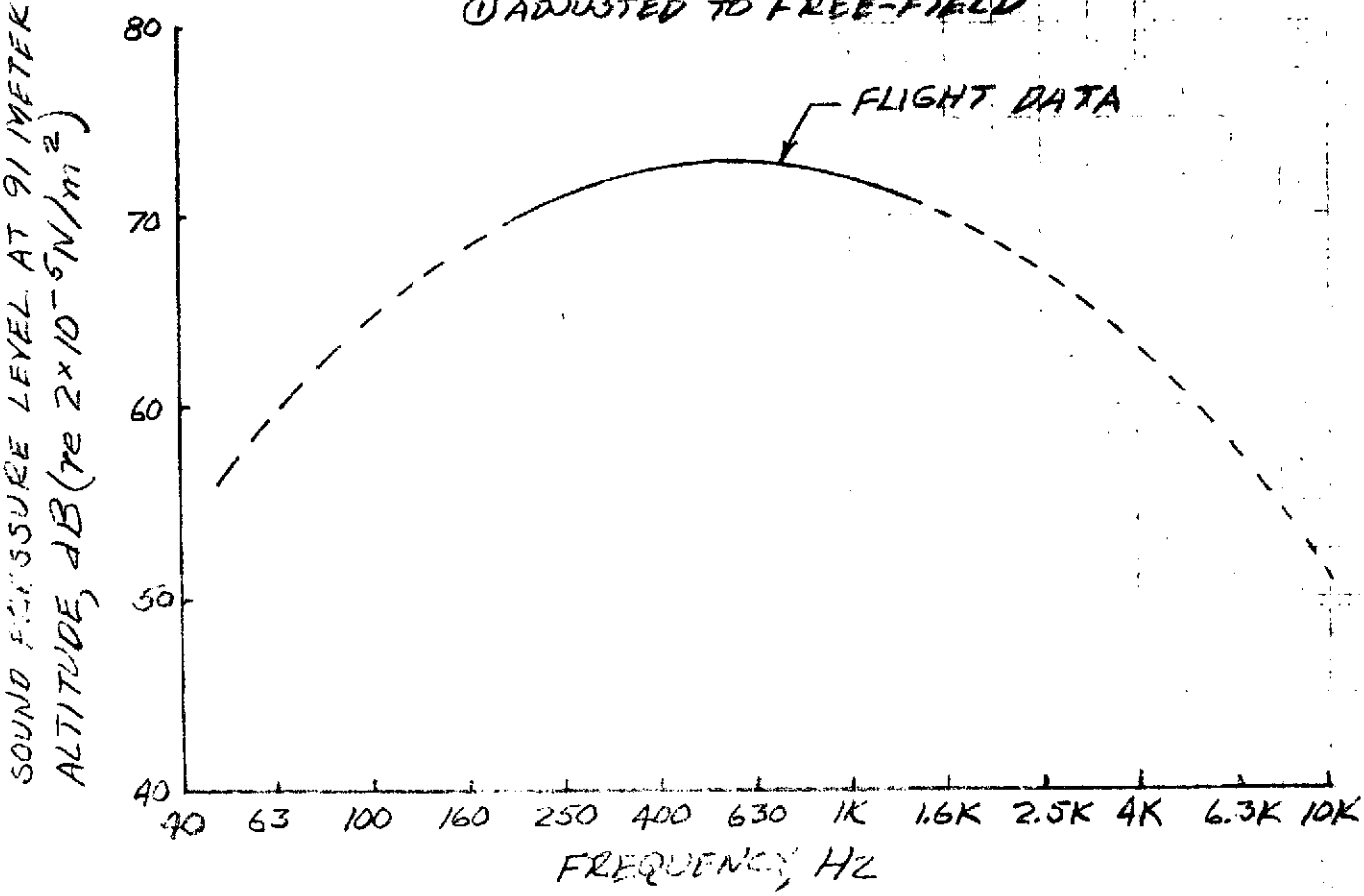

FIGURE 8. - COMPARISON OF MEASURED AIRFRAME NOISE WITH [illegible] FROM AN EXISTING EMPIRICAL RELATIONSHIP (REF. 2)

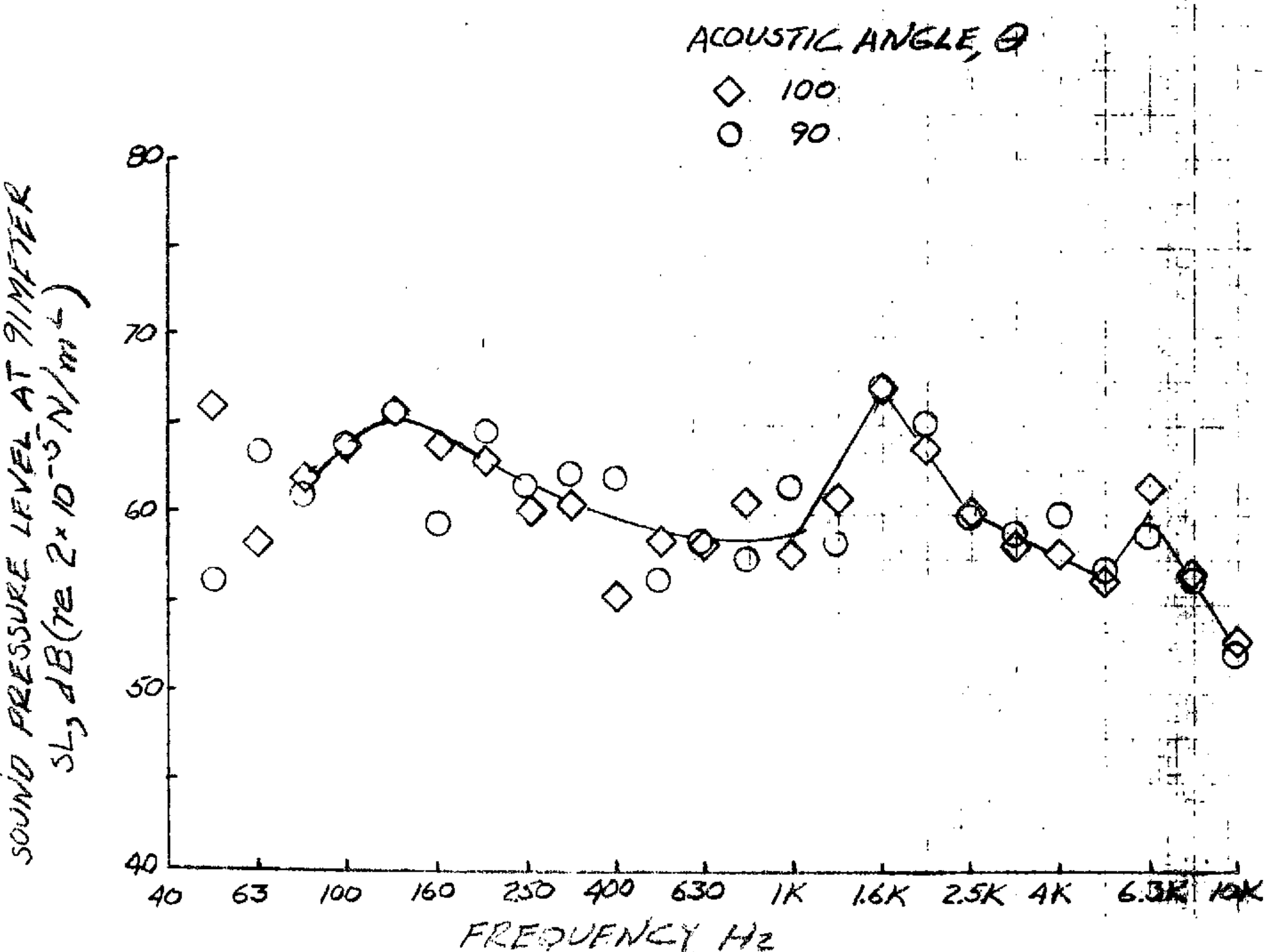

(a) J75 ENGINE NOISE (MEASURED STATICALLY AT IDLE)

FIGURE 9.- INFLUENCE OF J75 ENGINE NOISE ON AIRFRAME NOISE.

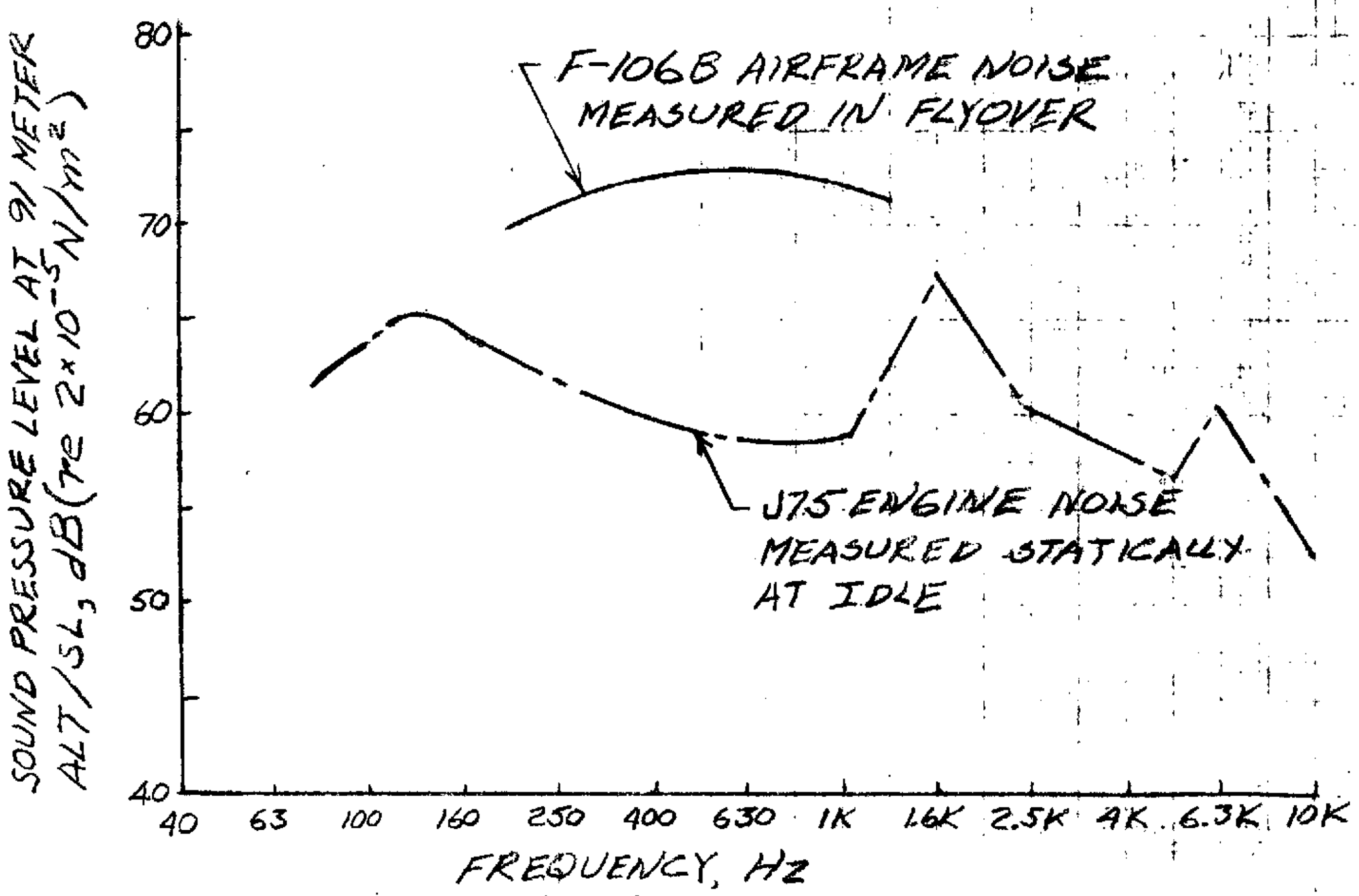

(b) COMPARISON OF NOISE LEVELS

FIGURE 9.- CONCLUDED

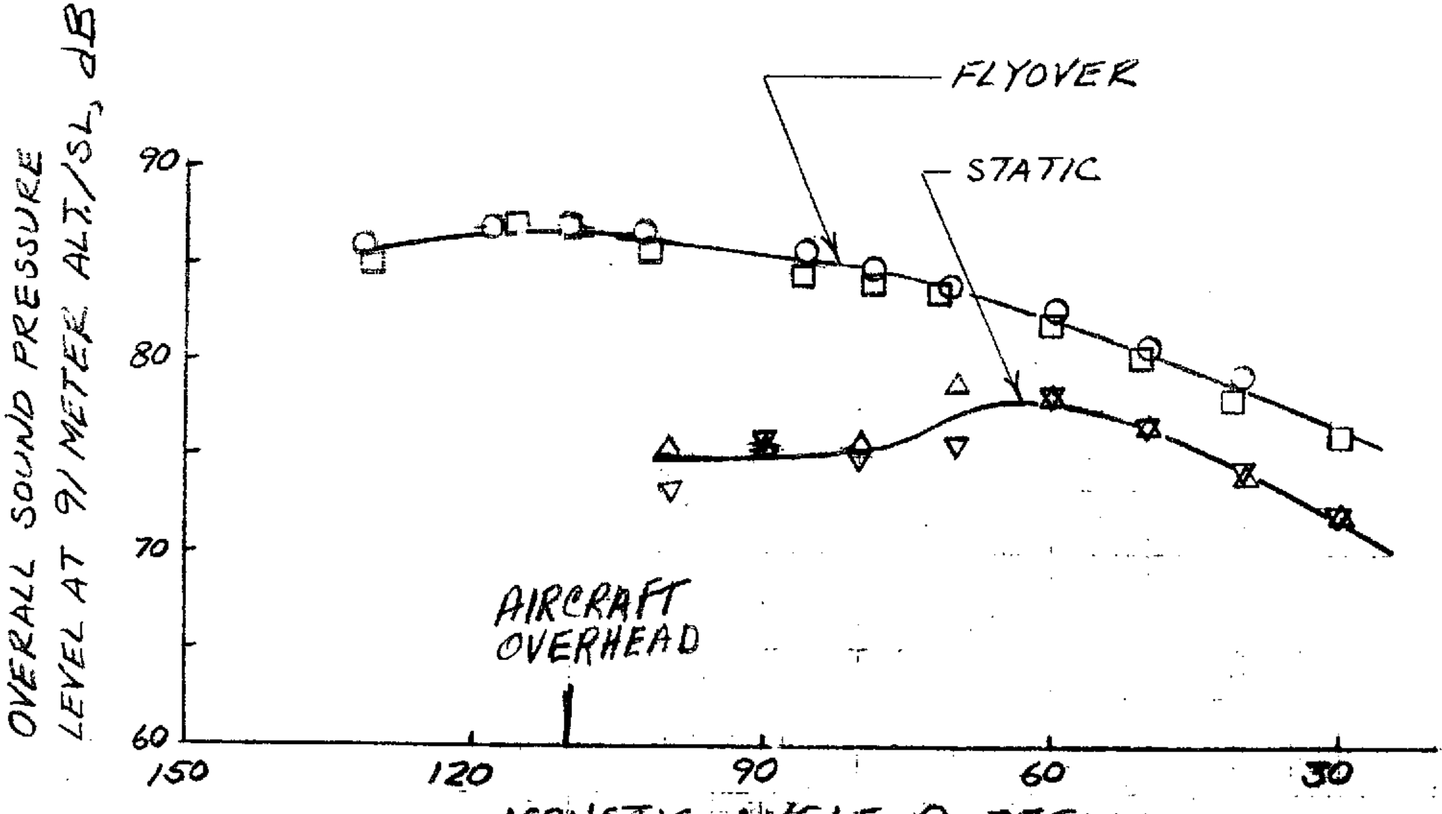

(a) OASPL

FIGURE 10.- FLYOVER AND STATIC NOISE DIRECTIVITY.

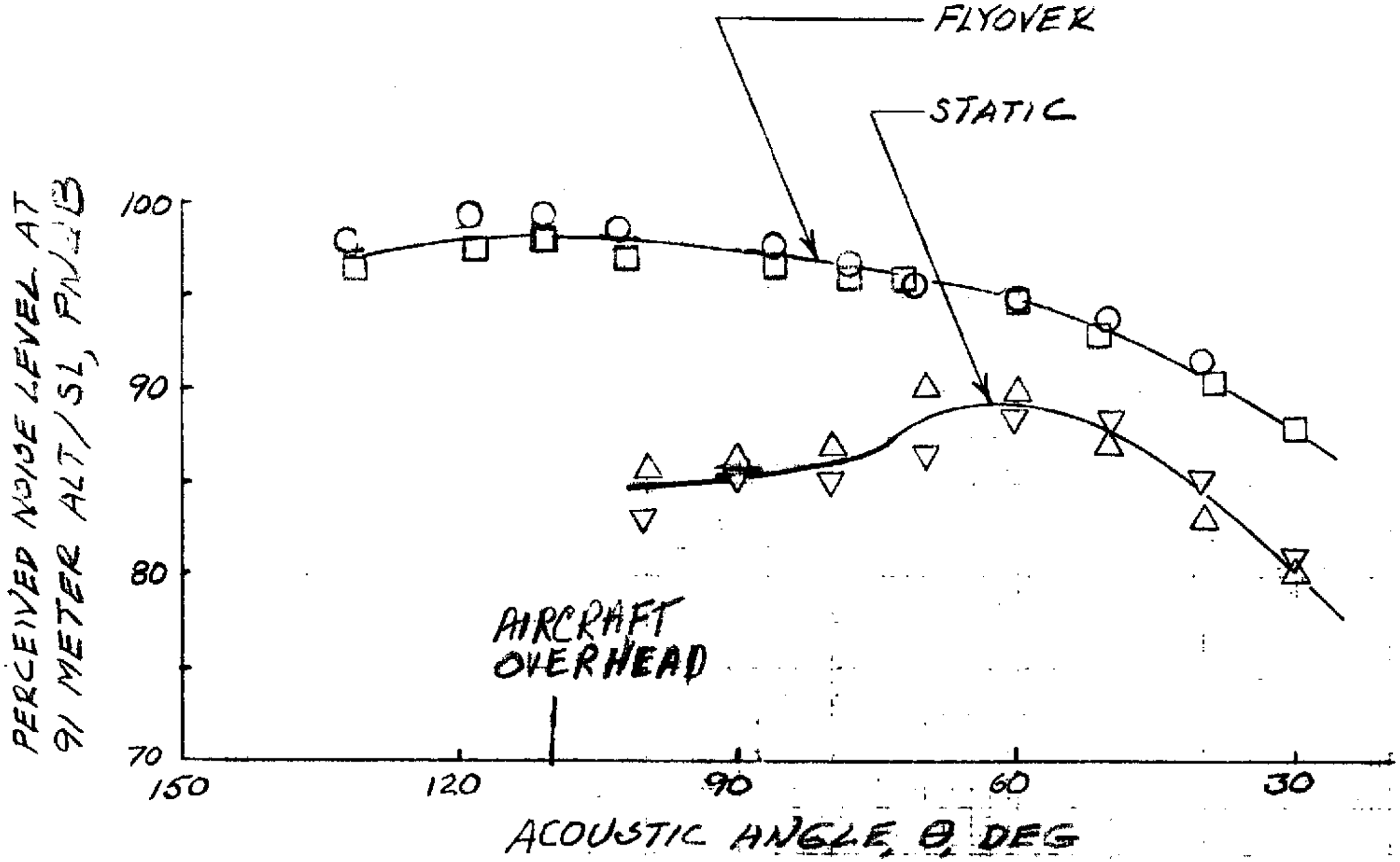

(b) PNL

FIGURE 14 - CONCLUDED.

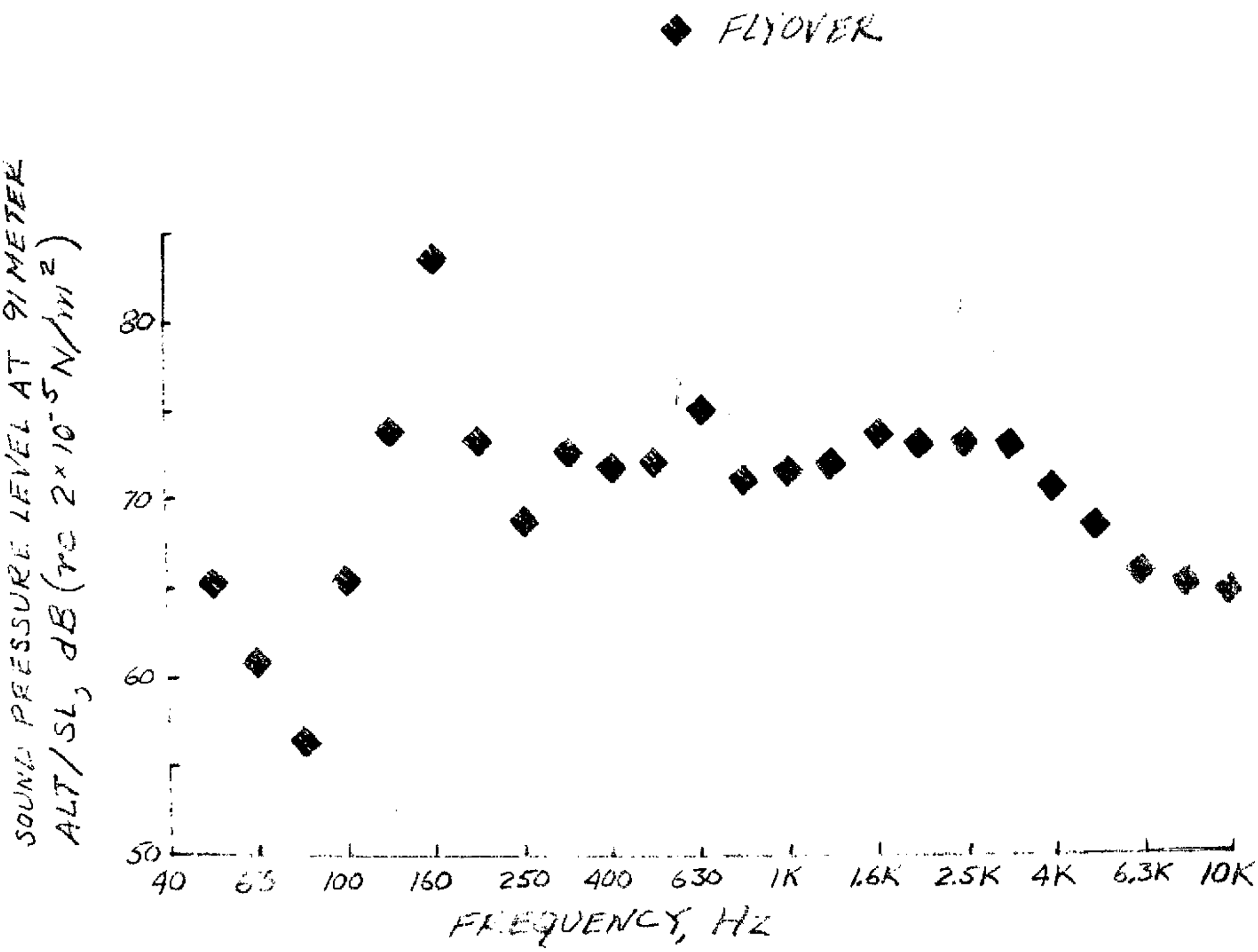

(a) $\theta = 120°$

FIGURE 11.- THIRD-OCTAVE BAND SPECTRA.

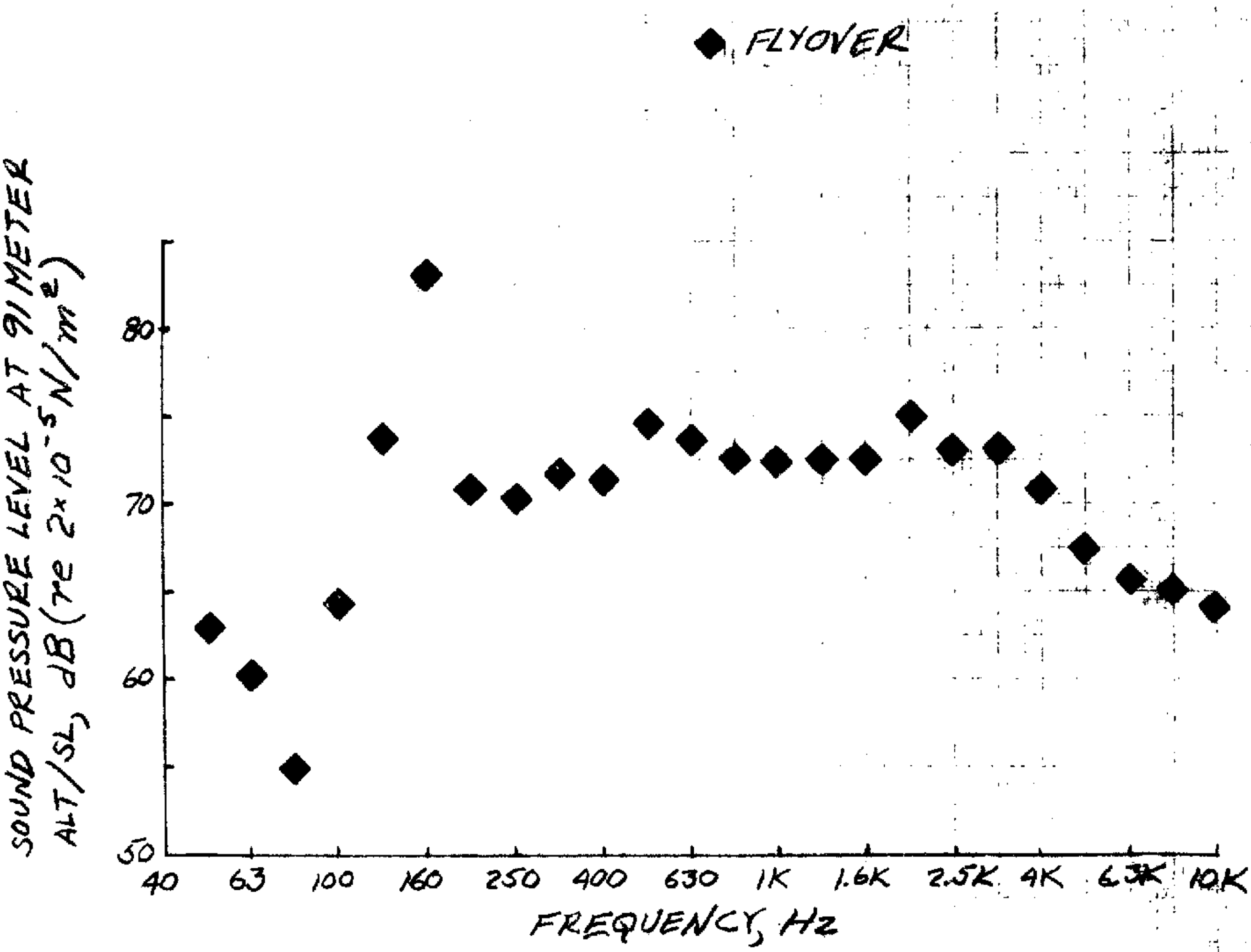

(b) $\theta = 110°$

FIGURE 16. - CONTINUED.

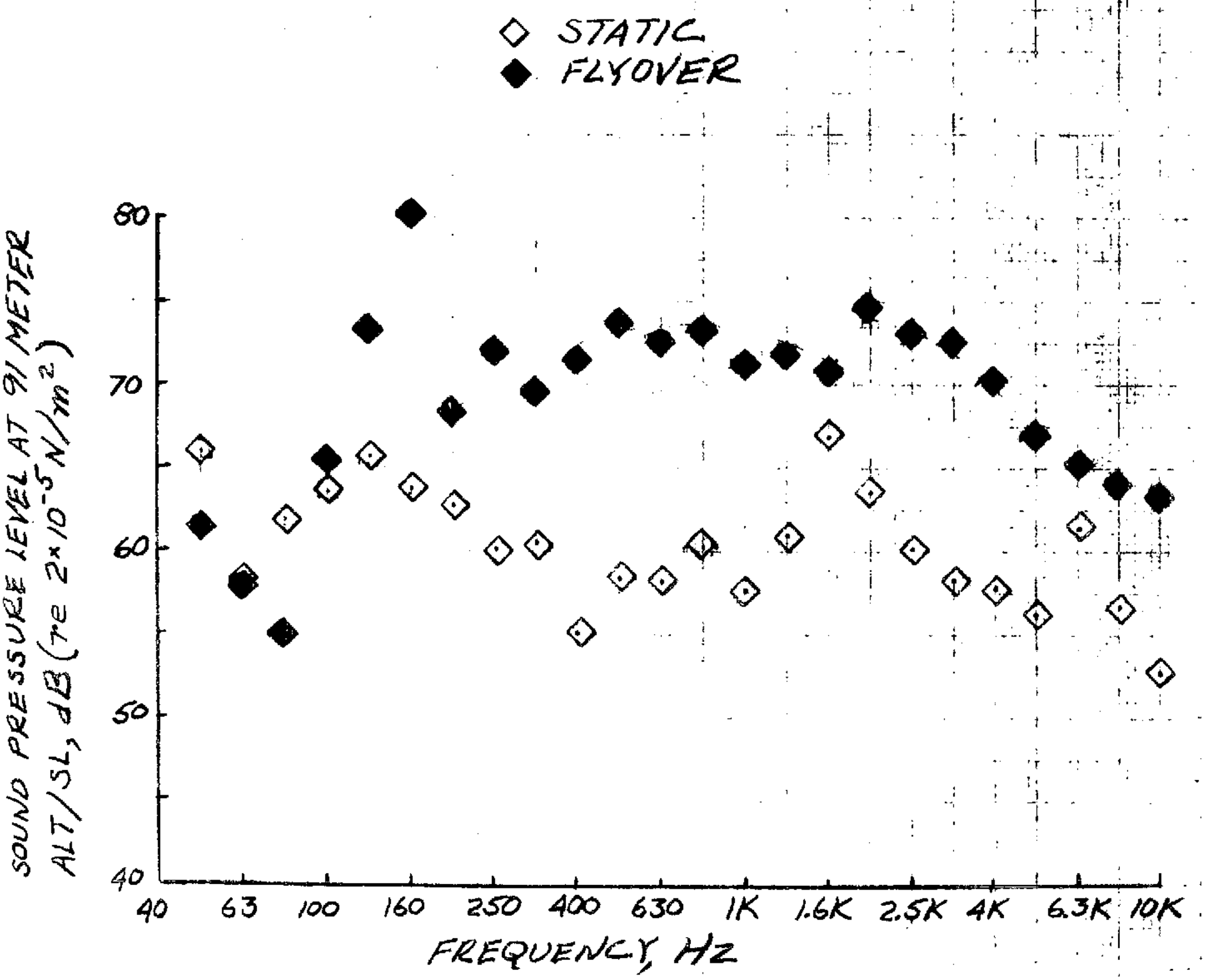

(c) $\theta = 100°$

FIGURE 11.- CONTINUED.

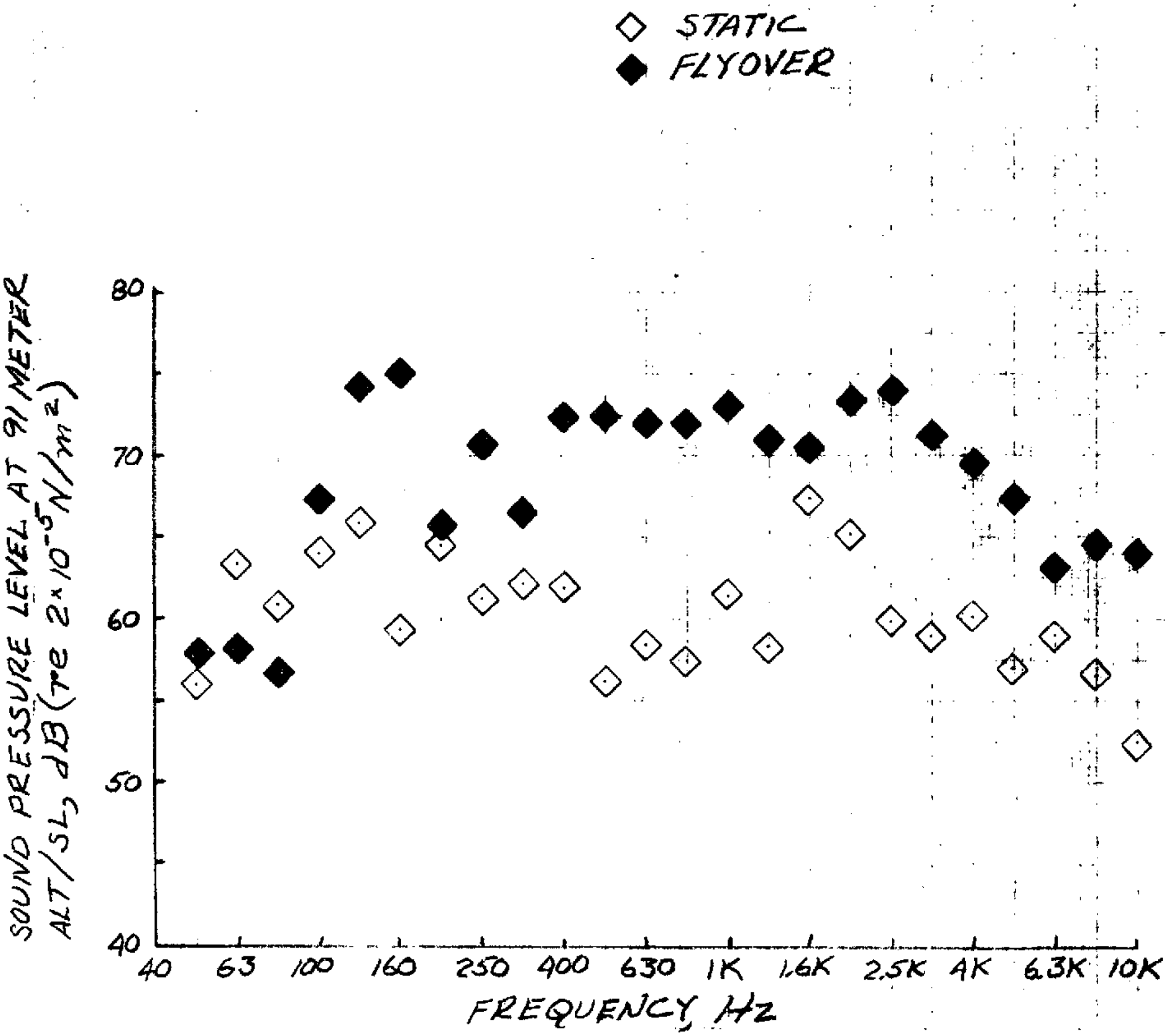

(d) $\theta = 90°$

FIGURE 1.1. - CONTINUED.

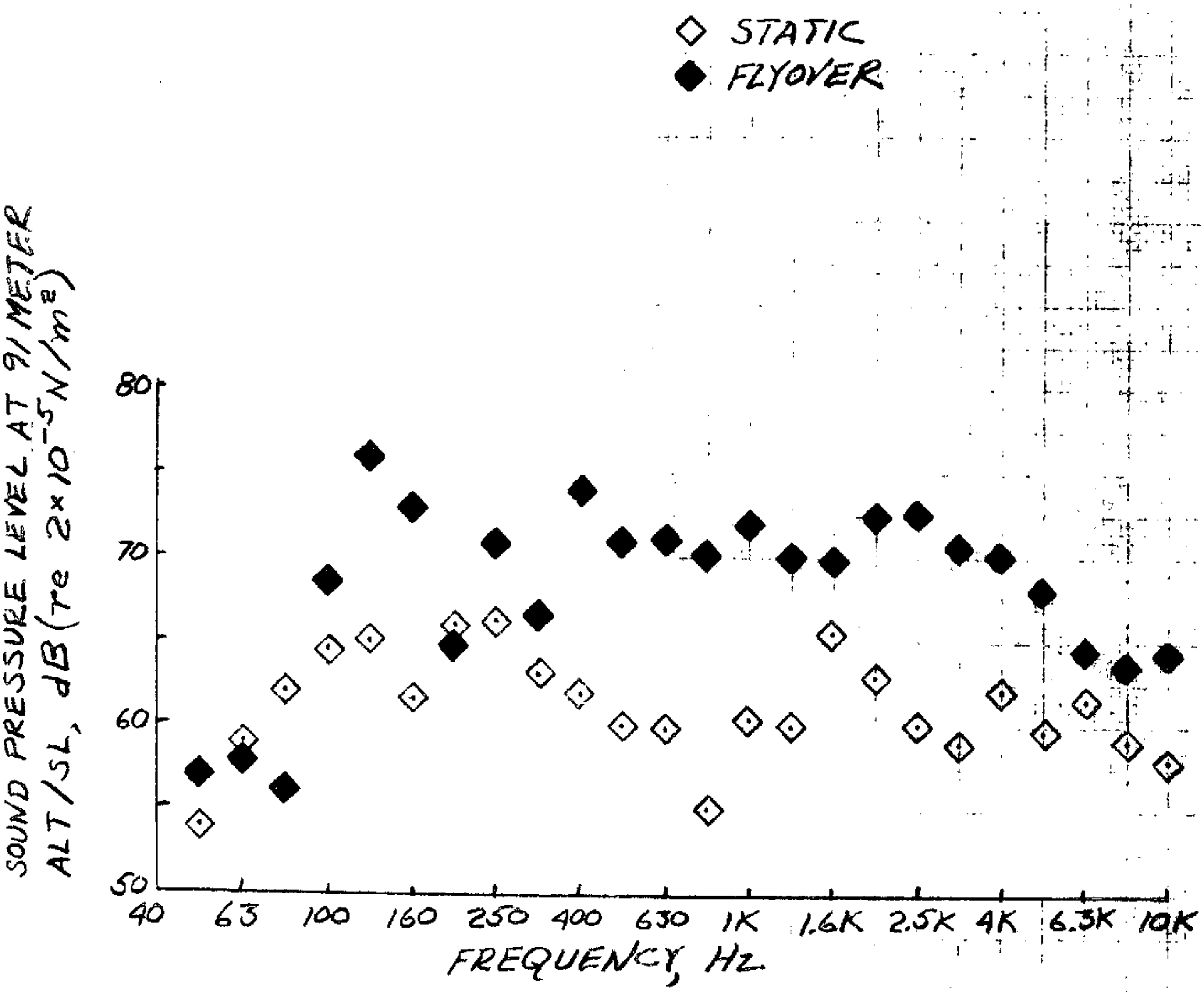

(e) $\theta = 80°$

FIGURE 11. - CONTINUED.

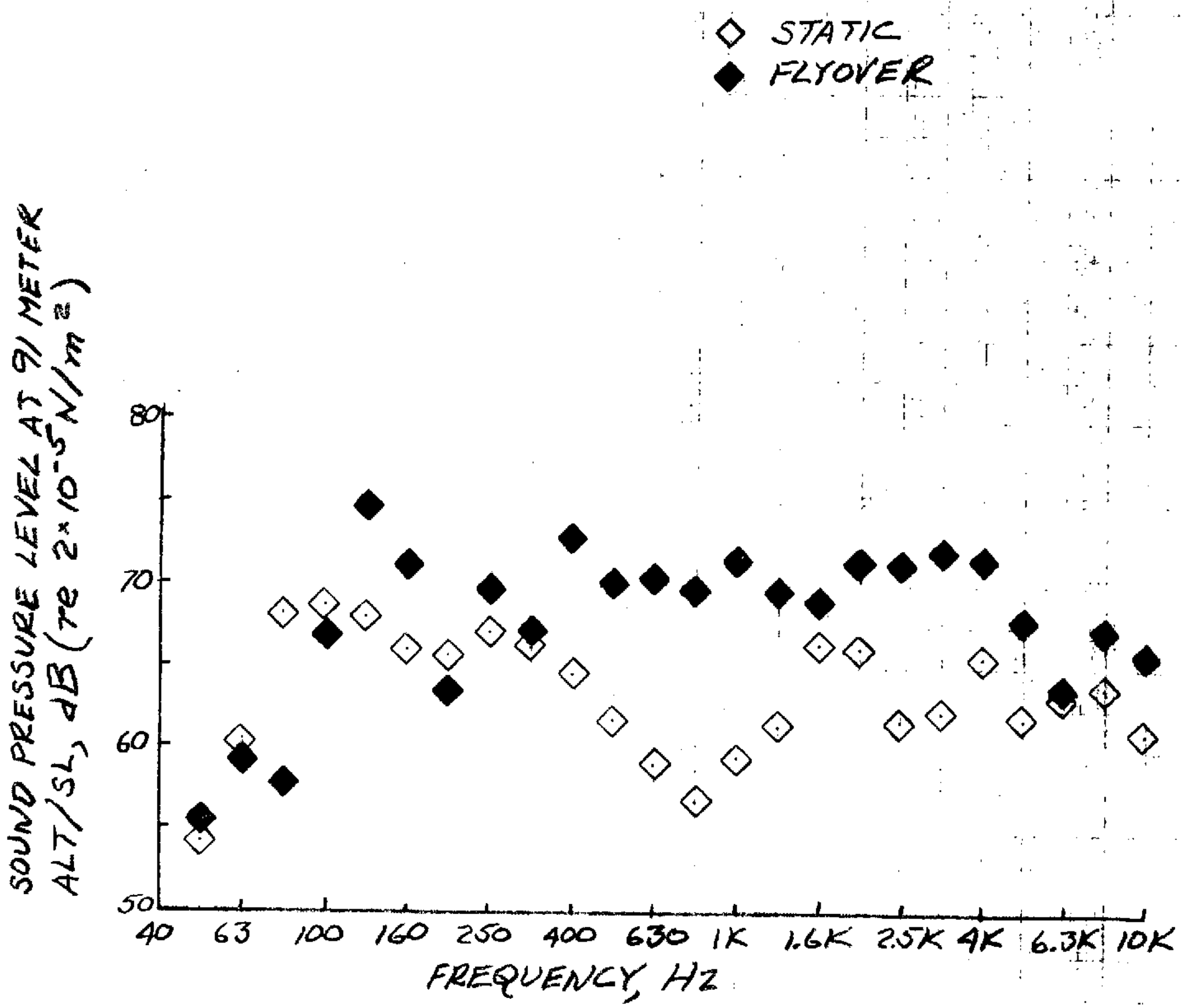

(f) $\theta = 70°$

FIGURE 11. - CONTINUED.

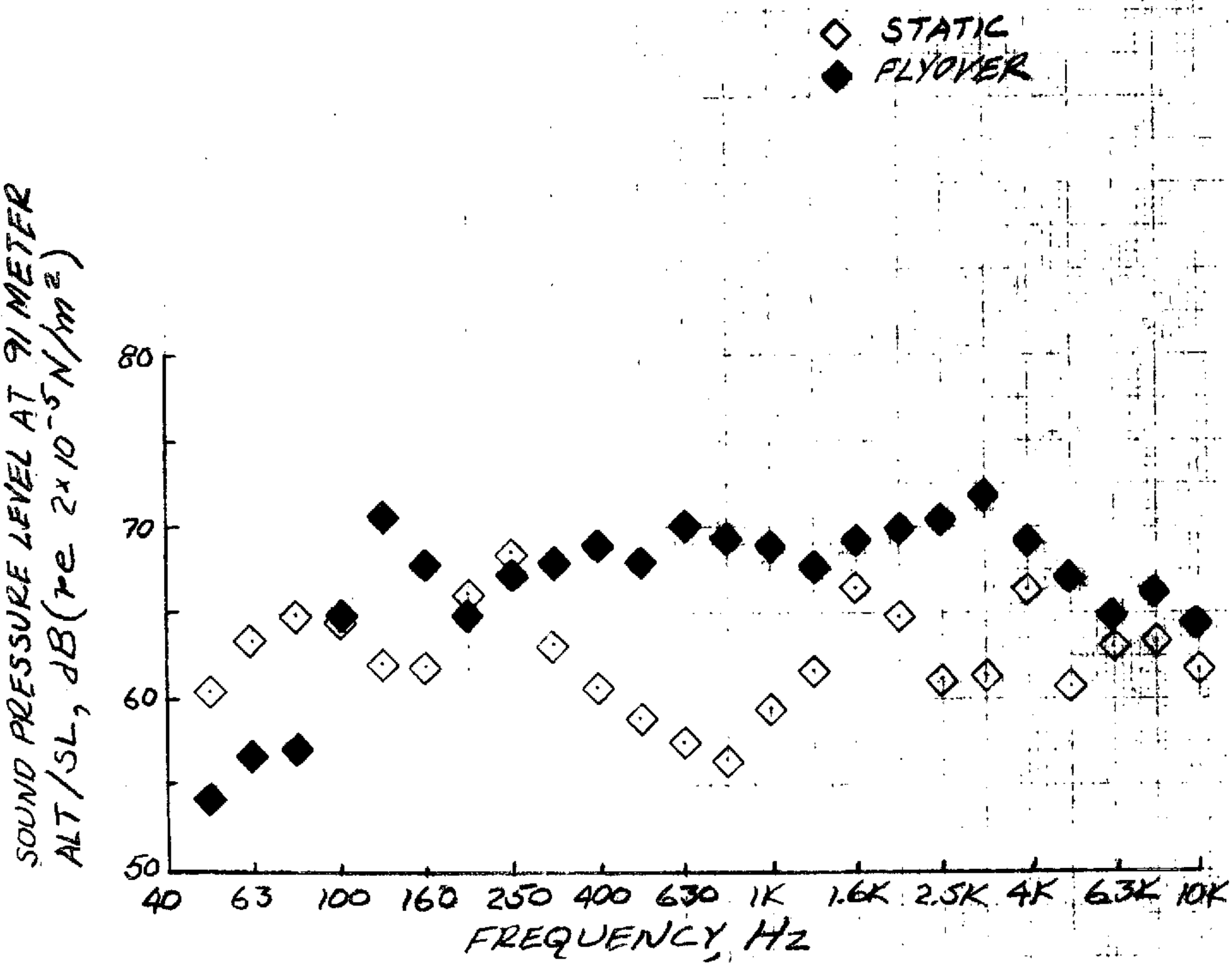

(g) $\theta = 60°$

FIGURE 11. - CONTINUED.

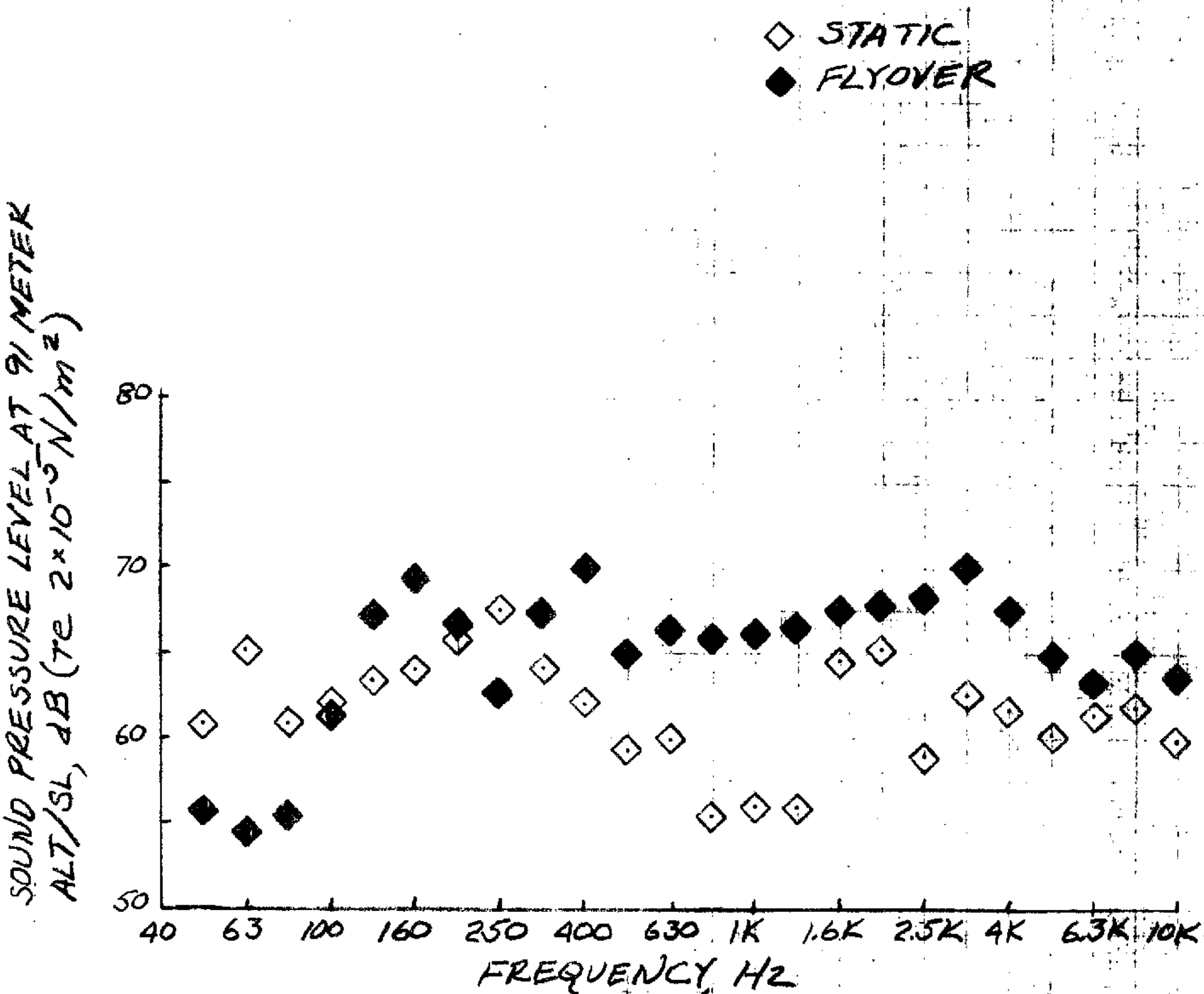

(h) θ = 50°

FIGURE 11.- CONTINUED.

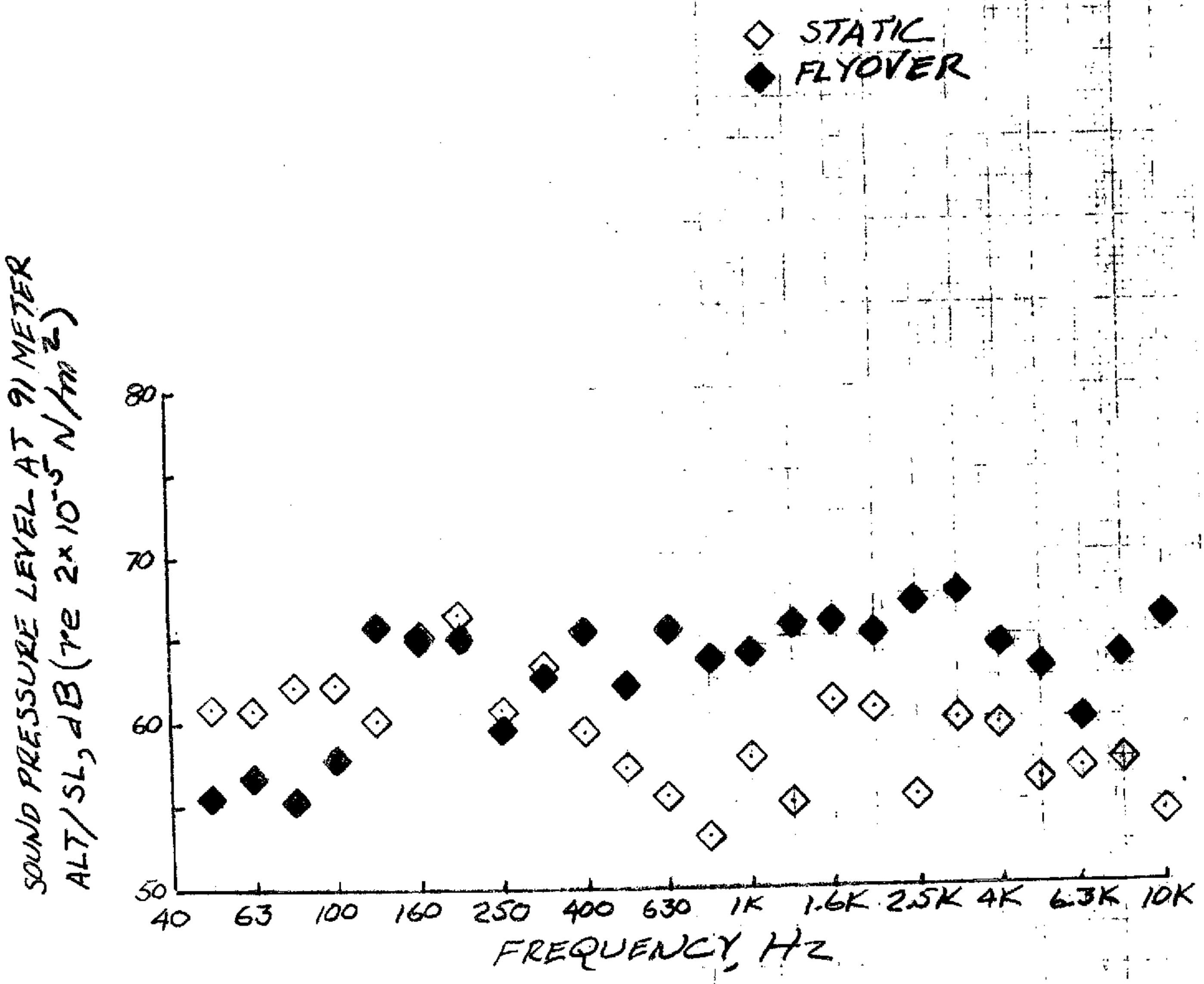

(i) $\theta = 40°$

FIGURE 11. - CONTINUED

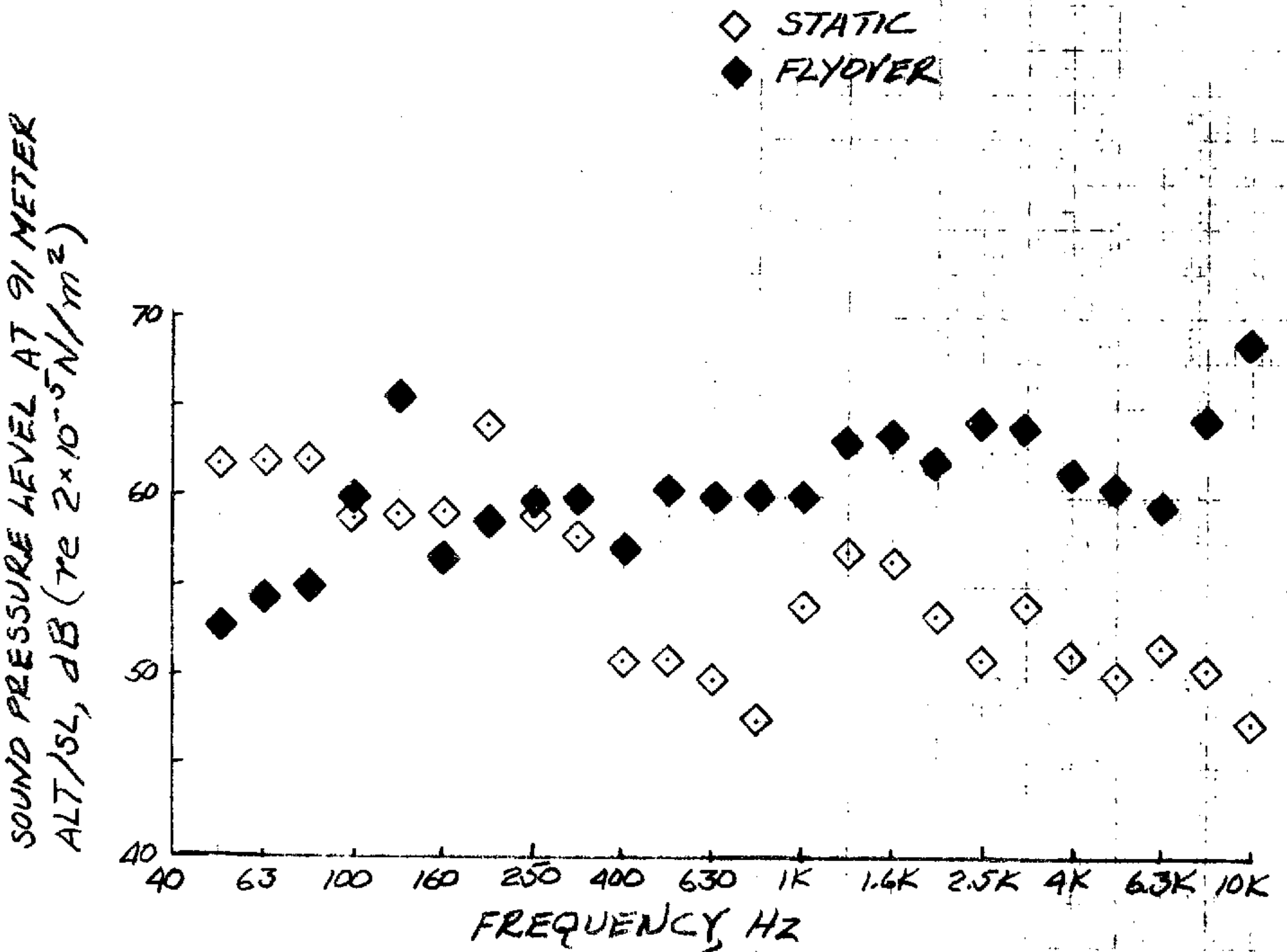

(g) $\theta = 30°$

FIGURE 11.- CONCLUDED